Marks Marinbahs

STUDY OF THE DYNAMICS, STRENGTH AND TECHNICAL CONDITION ASSESSMENT OF TRACTION ELECTROMECHANICAL EQUIPMENT

Summary of the Doctoral Thesis

RIGA TECHNICAL UNIVERSITY

Faculty of Mechanical Engineering, Transport and Aeronautics
Institute of Aeronautics

Marks Marinbahs

Doctoral Student of the Study Programme "Transport"

STUDY OF THE DYNAMICS, STRENGTH AND TECHNICAL CONDITION ASSESSMENT OF TRACTION ELECTROMECHANICAL EQUIPMENT

Summary of the Doctoral Thesis

Scientific supervisor
Professor Dr. habil. sc. ing.
VITĀLIJS PAVELKO
Scientific advisor
Docent Dr. sc. ing.
OĻEGS SĻISKIS

RTU Press
Riga 2023

DOCTORAL THESIS PROPOSED TO RIGA TECHNICAL UNIVERSITY FOR THE PROMOTION TO THE SCIENTIFIC DEGREE OF DOCTOR OF SCIENCE

To be granted the scientific degree of Doctor of Science (Ph. D.), the present Doctoral Thesis has been submitted for the defence at the open meeting of RTU Promotion Council on 17 February 2023, 13.00 at the Faculty of Mechanical Engineering, Transport and Aeronautics of Riga Technical University, 6b Kipsalas Street, Room 513.

OFFICIAL REVIEWERS

Professor Dr. sc. ing. Guntis Strautmanis,
Riga Technical University

Professor Dr. sc. Nadiia Bouraou
National Technical University of Ukraine, Ukraine

Professor Dh. D. Igor I. Tsukrov
University of New Hampshire, USA

DECLARATION OF ACADEMIC INTEGRITY

I hereby declare that the Doctoral Thesis submitted for the review to Riga Technical University for the promotion to the scientific degree of Doctor of Science is my own. I confirm that this Doctoral Thesis had not been submitted to any other university for the promotion to a scientific degree.

Marks Marinbahs …………………………. (signature)
Date: ………………………

The Doctoral Thesis has been written in English. It consists of an Introduction, 5 chapters, Conclusions, 78 figures, 28 tables; the total number of pages is 105, including appendices. The Bibliography contains 122 titles.

CONTENTS

GENERAL CHARACTERIZATION OF THE THESIS

Topic relevance

The actuality of the set task set also determines the constant increase in the operating speeds and loads of modern rolling stock, namely suburban and regional electric trains. In railway equipment, a traction electric drive is widely used, in most cases the elements of which, after installation, become inaccessible for direct control. There is a trend in the development and mass operation of electric trains with an asynchronous drive to improve performance in the intensification of traffic. In turn, the electric drive is an independent and complex system, since the processes occurring in it have a different physical nature. Therefore, in order to assess the technical condition of the mechanical and electrical elements of electromechanical equipment, as well as to control its technical condition, it is advisable to carry out comprehensive tests when putting the equipment into operation. The foregoing is especially relevant for new products as well as at the stage of acceptance testing of serial products.

Currently, methods for diagnosing the mechanical part of the electric drive based on vibration and acoustic parameters are widely used. Methods for electrical control of motors based on the consumed current are being developed. The main drawback of the existing methods of separate control of mechanical and electromechanical units is that they do not take into account the interconnection and interdependence of the total operation of the drive elements, in particular the motor and gearbox, which are often checked separately.

The aim of the Doctoral Thesis

The aim of the Doctoral Thesis is to study the possibilities of the dynamics, strength and technical condition assessment of traction electromechanical equipment in industrial and continuous production conditions and to improve the completeness and efficiency of pre-operational test trials based on the creation of a methodology for an integrated approach to the control and analysis of the mechanical strength and vibration activity of traction equipment.

To achieve the aim, the following tasks have been solved:

1. Development of a methodology for comprehensive analysis of the design of electromechanical equipment based on its operating conditions.
2. Development and implementation of a methodology for determining the safety margin of the equipment taking into account the mechanical loads of the drive.
3. Analysis of the influence of defects in equipment units on the change in diagnostic parameters and the establishment of links between them.
4. Practical approbation of the technique for monitoring the technical condition of electromechanical equipment based on its vibration activity.

To solve the tasks, an analysis of the work on the creation of methods, techniques and systems for non-destructive testing and diagnostics of electromechanical equipment was carried out.

The study of methods and models of non-destructive testing of mechanical and electromechanical equipment based on vibration analysis is the subject of many research papers. However, in these studies, methods and techniques for monitoring and predicting the

service life of units based on mechanical parameters are mainly presented. Little attention has been paid to controlling the vibration of mechanical components in the drive.

Scientific novelty of the Thesis

1. A methodology for assessing the technical condition of electromechanical equipment units has been developed taking into consideration the analysis of mechanical parameters as part of a real traction electric drive. Mechanical diagnostic parameters are the general level of vibration acceleration and vibration velocity.
2. Based on the established connection between diagnostic signs and the type of defect or malfunction, an approach is proposed for its detection.
3. A methodology for estimating the safety margin of electromechanical equipment is proposed, which has the most sensitive diagnostic features with the possibility of estimating the safety margin of the equipment under conditions of changing external loads.

Theoretical and practical significance of the Thesis

The theoretical and practical significance of the work lies in the fact that a method for monitoring the technical condition of electromechanical equipment has been developed and tested, which increases its reliability and efficiency. This will make it possible to switch to automated control of the actual state of traction electrical equipment. Based on the results of the study, the methodology and means are proposed for monitoring the technical condition of motor-gear units produced by JSC "Rīgas elektromašīnbūves rūpnīca" used on suburban motor car bogies with a design speed of up to 160 km/h.

Research methods, reliability and validity of results

The present research is based on the results of theoretical and experimental developments, which are presented in five chapters.

In Chapter 1, on the basis of research, an overview of existing methods and techniques for monitoring and diagnosing the technical condition of electromechanical equipment is given. The standards for vibration control are also considered.

Chapter 2 analyses the existing methods for processing diagnostic signals as well as signs of manifestation of defects in the main units. The object of control is also considered: the motor-reducer block of the motor car of the electric train. The main attention is paid to the development of a methodology for the integrated control of electromechanical equipment, including a model and algorithm for the operation of an information-measuring system for monitoring the technical condition, a model and algorithm for estimating the resource of equipment.

Chapter 3 presents the development of a virtual and physical test and measurement system, including a description of the subject of research and a description of the drive control system. A model is presented to determine the critical points of maximum structural stress. The main attention is paid to the development of a methodology for the integrated control of electromechanical equipment, including a model and algorithm for the operation of an

information-measuring system for monitoring the technical condition, a model and algorithm for estimating the resource of equipment.

Chapter 4 presents the results of the analysis of the influence of the loading of the object under study on the change in diagnostic parameters based on an experimental study of the methodology and means of monitoring the technical condition of the equipment. The model for predicting the safety margin of the equipment has been experimentally tested.

Chapter 5 describes the practical application of the methodology in the production environment of JSC "Rīgas elektromašīnbūves rūpnīca". The data of the control object (geared motor units of passenger electric trains used on the bogies of motor cars of passenger electric trains) were collected and analysed and the most vulnerable segments of the structure requiring direct monitoring of their condition were identified.

The research is based on:

1) the method for determining mechanical loads and assessing the safety margin of the supporting structures of traction motor-reduced units and the method for evaluating the operation of electromechanical equipment based on the relationship, interaction and subsequent joint analysis of the vibration parameters of the equipment;

2) the structure and hardware-software implementation of bench testing of equipment to identify the technical condition of electromechanical equipment;

3) the results of an experimental study confirming the possibility of increasing the efficiency of the process of conducting acceptance tests and evaluating the safety margin of electromechanical equipment through the integrated use of vibration and energy parameters.

Approbation of the results

The results of the Thesis were presented in the following scientific conferences:

1. IEEE 59th International Scientific Conference on Power and Electrical Engineering of Riga Technical University (RTUCON 2018), presentation: Investigation of Autonomous Traction Motor Dynamic Using Method of Mutual Loading and Computer Simulation. Riga, Latvia, IEEE, 2018.

2. 16th Conference on Electrical Machines, Drives and Power Systems (ELMA 2019), presentation: Investigation of Traction Motor Dynamic Using Computer Simulation and Method of Mutual Loading of Two Pair Motors. Varna, Bulgaria, IEEE, 2019.

3. 16th Conference on Electrical Machines, Drives and Power Systems (ELMA 2019), presentation: Investigation of Electrical Bus Traction Motor Dynamic Using Methods of Physical and Computer Simulation. Varna, Bulgaria, IEEE, 2019.

4. 17th Conference on Electrical Machines, Drives and Power Systems (ELMA 2021), presentation: Carrying out of Tests for the Functionality of the Traction Autonomous Drives in the Conditions of Industry and Serial Production. Sofia, Bulgaria, IEEE, 2021.

5. 17th Conference on Electrical Machines, Drives and Power Systems (ELMA 2021), presentation: Carrying out of Strength Tests of Geared Motor Box as Part of a Frequency-Controlled Traction Electric Drive. Sofia, Bulgaria, IEEE, 2021.

6. IEEE 62nd International Scientific Conference on Power and Electrical Engineering of Riga Technical University (RTUCON 2021), presentation: Determination of the Level of Own Vibration of Geared Motor Boxes in Industrial Conditions. Riga, Latvia, IEEE, 2021.

7. 9th International Conference on Electrical and Electronics Engineering (ICEEE 2022), presentation: Carrying Out of Strength Control of Mutual Loaded Traction Geared Motor Boxes as a Part of Industrial Tests. Alanya, Turkey, IEEE, 2022.

8. 8th International Youth Conference on Energy (IYCE 2022), presentation: Determination of the Strength Characteristics of Traction Gears under Shock Loads. Eger, Hungary, IEEE, 8 July 2022.

9. 2nd International Conference on Electrical, Computer and Energy Technologies (ICECET 2022), presentation: Evaluation of the Strength of Traction Geared Motor Units by Permissible Stresses and the Level of Vibration Activity. Prague, Czech Republic, IEEE, 21 July 2022.

The results of the Thesis, were presented in the following scientific papers:

1. Dvorņikovs, I., Marinbahs, M., Sliskis, O., Ketners, K. Investigation of Autonomous Traction Motor Dynamic Using Method of Mutual Loading and Computer Simulation. In: *2018 IEEE 59th International Scientific Conference on Power and Electrical Engineering of Riga Technical University (RTUCON 2018): Conference Proceedings*, Latvia, Riga, 12–14 November 2018. Piscataway: IEEE, 2018, ISBN 978-1-5386-6904-4. e-ISBN 978-1-5386-6903-7. *Available from: doi:10.1109/RTUCON.2018.8659827*

2. Dvornikovs, I., Marinbahs, M., Zarembo, J., Groza, E., Ketners, K. Investigation of Traction Motor Dynamic Using Computer Simulation and Method of Mutual Loading of Two Pair Motors. In: *2019 16th Conference on Electrical Machines, Drives and Power Systems (ELMA 2019)*, Bulgaria, Varna, 6–8 June 2019. Piscataway: IEEE, 2019, ISBN 978-1-7281-1414-9. e-ISBN 978-1-7281-1413-2. *Available from: doi:10.1109/ELMA.2019.8771668*

3. Sliskis, O., Dvornikovs, I., Marinbahs, M., Marks, J., Groza, E. Investigation of Electrical Bus Traction Motor Dynamic Using Methods of Physical and Computer Simulation. In: *2019 16th Conference on Electrical Machines, Drives and Power Systems (ELMA 2019)*, Bulgaria, Varna, 6–8 June 2019. Piscataway: IEEE, 2019, ISBN 978-1-7281-1414-9. e-ISBN 978-1-7281-1413-2. *Available from: doi:10.1109/ELMA.2019.8771668*

4. Dvornikovs, I., Marinbahs, M., Kobenkins, G., Sliskis, O., Ketners, K. Carrying out of Tests for the Functionality of the Traction Autonomous Drives in the Conditions of Industry and Serial Production. In: 2021 17th Conference on Electrical Machines, Drives and Power Systems (ELMA 2021), Bulgaria, Sofia, 1–4 July 2021. Piscataway: IEEE, 2021, pp.189–192. ISBN 978-1-6654-1186-8. e-ISBN 978-1-6654-3582-6. *Available from: doi:10.1109/ELMA52514.2021.9503099*

5. Kobenkins, G., Marinbahs, M., Burenin, V., Zarembo, J., Sļiskis, O. Carrying out of Strenght Tests of Geared Motor Box as Part of a Frequency-Controlled Traction Electric Drive. In: *2021 17th Conference on Electrical Machines, Drives and Power Systems (ELMA 2021)*, Bulgaria, Sofia, 1–4 July 2021. Piscataway: IEEE, 2021, pp. 185–188. ISBN 978-1-6654-1186-8. e-ISBN 978-1-6654-3582-6. *Available from: doi:10.1109/ELMA52514.2021.9502985*

6. Kobenkins, G., Marinbahs, M., Zarembo, J., Burenin, V., Bizans, A., Sliskis, O. Determination of the Level of Own Vibration of Geared Motor Boxes in Industrial Conditions. In: *2021 IEEE 62nd International Scientific Conference on Power and Electrical Engineering of Riga Technical University (RTUCON 2021)*, Latvia, Riga, 15–

17 November 2021. Piscataway: IEEE, 2021, ISBN 978-1-6654-3805-6. e-ISBN 978-1-6654-3804-9. *Available from: doi:10.1109/RTUCON53541.2021.9711589*

7. Kobenkins, G., Marinbahs, M., Bizans, A., Rilevs, N., Burenin, V., Sliskis, O. Carrying Out of Strength Control of Mutual Loaded Traction Geared Motor Boxes as a Part of Industrial Tests. In: *2022 9th International Conference on Electrical and Electronics Engineering (ICEEE 2022)*, Turkey, Alanya, 29–31 March 2022. Piscataway: IEEE, 2022, pp.185–189. ISBN 978-1-6654-6755-1. e-ISBN 978-1-6654-6754-4. *Available from: doi:10.1109/ICEEE55327.2022.9772530*

8. Marinbahs, M., Kobenkins, G., Pavelko, V., Bizans, A., Rilevs, N., Sliskis, O. Determination of the Strength Characteristics of Traction Gears Under Shock Loads. In: *The 8th International Youth Conference on Energy (IYCE-2022),* 6–9 July 2022, Eger, Hungary. *Available from: doi: 10.1109/IYCE54153.2022.9857535*

9. Kobenkins, G., Marinbahs, M., Bizans, A., Rilevs, N., Burenin, V., Sliskis, O. Evaluation of the Strength of Traction Geared Motor Units by Permissible Stresses and the Level of Vibration Activity. In: *Proc. of the International Conference on Electrical, Computer and Energy Technologies (ICECET 2022),* 20–22 July 2022, Prague, Czech Republic. *Available from: doi: 10.1109/ICECET55527.2022.9872590*

10. Kobenkins, G., Marinbahs, M., Bizans, A., Rilevs, N., Sliskis, O. The influence of dynamic loads on the vibration level of rotating units of traction drives. In: *Proc. 3rd International Conference on Power, Energy and Electrical Engineering (PEEE2022),* November 18–20, 2022, Barcelona, Spain.

11. Kobenkins, G., Marinbahs, M., Bizans, A., Sliskis, O. Verification of Strength Characteristics of Traction Geared Motor Unit on Industrial Conditions. In: *Proc. of the 25th International Conference on Electrical Machines and Systems (ICEMS2022),* 29 November – 2 December 2022, Chiang Mai, Thailand.

12. Kobenkins, G., Marinbahs, M., Bizans, A., Sliskis, O. Strength and Vibration Activity Control of Traction Geared Motor Units. In: *Proc. of the 25th International Conference on Electrical Machines and Systems (ICEMS2022),* 29 November – 2 December 2022, Chiang Mai, Thailand.

CHAPTER 1. STATUS ANALYSIS AND DIRECTIONS OF RESEARCH

1.1. Determination of the reliability of traction machines and equipment at the stage of industrial testing

The economic efficiency of machines and equipment directly depends on their technical condition. At present, two types of equipment maintenance have become widespread in enterprises: maintenance after failure and maintenance according to the regulations. However, this leads, on the one hand, to a significant underutilization of the resource of the structures of the units and the machine as a whole, and, on the other hand, does not adequately ensure their reliability. In an unforeseen breakdown, the enterprise incurs significant economic costs. In the second case, when maintenance is carried out according to the regulations, this also leads to additional costs. This is due to the fact that any "movement" violates the quality of the kinematic relationships in the mechanism achieved by the natural running-in of mating components and parts during operation.

In particular, the most important condition for the efficient operation of transport equipment (in particular, railway transport) is the trouble-free operation of its subsystems, the main of which is traction electrical equipment. One of the possible ways to maintain a high level of system reliability is the use of methods, techniques and means of non-destructive testing. The use of complex methods and techniques for assessing the performance of objects and their technical implementation is an urgent task, since its solution will improve the overall efficiency of the equipment. Traction drive is a system consisting of mechanical and electrical subsystems together with a control system.

Defects in the electrical subsystem are defects in drive motors. The most common defects of electric motors (asynchronous motor is considered in this PhD work) are: operation of the electric motor in two phases; interturn circuit; overload and overheating of the motor stator; rotor imbalance; breakage or loosening of the fastening of the rods in the squirrel cage; uneven air gap between the stator and rotor; damage to the stator windings or insulation; and loosening of the stator windings [1]–[4].

In this dissertation, an object consisting of an electric motor and a mechanical transmission – a traction geared motor unit (hereinafter referred to as MGU) – was investigated, since it is a typical electromechanical equipment.

1.2. Overview of existing methods and techniques for monitoring and diagnosing the technical condition of electromechanical equipment

At present, much attention is paid to the control and diagnostics of complex technical systems. This is evidenced by a large number of publications and the refinement of international standards ISO/TC 108 "Vibration and shock" (ISO 17359:2003, ISO 13380:2002, ISO 13379:2003, ISO 10816-6:1995, ISO 13373-1:2002, ISO/DIS 13373-2, ISO/DIS 15242-1, ISO 13374-1:2003) [5]–[10].

Any control and diagnostic system operates on the principle of deviations (the Salisbury principle). The difference between the actual and reference value of the diagnostic parameters is calculated, which is called the diagnostic symptom. The error with which the value of a diagnostic symptom is estimated largely determines the quality and reliability of the diagnosis and prognosis of the controlled object.

Monitoring and diagnostics should solve the problem of assessing the actual state of objects in the process of operation and provide information for organizing the repair cycle.

The appearance or development in time of a particular defect leads to a redistribution of energy between the components of the spectrum of the resulting oscillatory process. Knowledge of the physical features and regularities of the processes of oscillation initiation in the structures of an electromechanical system allows one to qualitatively identify diagnostic features, the change of which unambiguously indicates specific faults (the initiation and development of defects in one or another kinematic pair of an electromechanical system) and allows them to be assessed.

1.3. Features of the control of electromechanical equipment with operating processes of various physical nature

The traction electric drive is a technical system used to convert electrical energy into mechanical energy in order to set the working body of the machine in motion. In this case, the electric drive also performs the function of controlling this movement. Thus, the indicated transformation of the two types of energy is interconnected.

The fluctuations of physical parameters arising in the system (changes in power, forces, moments, speeds, accelerations), generated both by external influences and by developing defects in the electromechanical part of the system, are mutually reflected in the mechanical and electrical characteristics. This is also indirectly reflected in the diagnostic signals generated by these phenomena of various physical nature.

These changes are associated with the electromagnetic torque of the motor, which is determined by the value of the current consumed, the voltage of the phases and the state of the material of the rotor, stator, friction conditions in the supports and the amount of slip.

The following methods of digital signal processing are currently widely used in practice to control the TS of equipment in the field of vibration diagnostics: PIC factor, according to the spectrum of the vibration signal, according to the spectrum of the envelope, and the method of shock pulses. The method of vibration control by the spectrum of the vibration signal is usually considered by practical diagnosticians to be the main, the most effective one [3].

Current based control can be implemented on most machines by using current transformers that are installed in the inverter. The use of current signals is convenient when controlling a large number of motors. In addition, the type of faults in the current signal is uniform and is not affected by external factors [11].

Thus, the analysis of the consumed current is currently a promising method for assessing the condition of both the electric motor and mechanical equipment.

Studies [11] and [12] have shown that each type of fault is associated with a corresponding frequency component in the stator phase current. For example, the frequency components of the stator current of an induction motor can be divided into two separate groups:

1) spectral components: excitation frequencies, supply harmonics; spatial harmonics associated with the spatial arrangement of the winding;
2) abnormal spectral components: as a result of stator malfunctions; incorrect installation; load change.

The main features of the control of the electric drive of railway vehicles are:

1) a set of MGU of the same composition (4 MGU per section);
2) change in the external load of the MGU due to the heterogeneity of the track (including movement up and down), as well as uneven loading (in terms of the number of passengers, etc.);
3) checking the status of the most critical nodes is carried out periodically in the depot according to a certain regulation.

The use of methods and techniques of vibration control for an electric drive of a railway vehicle (MGU) moving along rails is associated with the need to isolate a useful diagnostic signal from a variety of interference caused, for example, by the imposition of impacts on bearing supports from rail irregularities and other sources.

1.4. Main results and conclusions of Chapter 1

1. Various methods, techniques, models and algorithms are used to control equipment. Vibration control systems are the most common.
2. In turn, the electric drive is an independent and complex system, since the processes occurring in it have a different physical nature. Therefore, to assess the technical condition of the mechanical and electrical elements of electromechanical equipment, it is advisable to use complex monitoring tools.
3. A review of existing diagnostic methods, techniques and complexes and standards created on their basis shows a high level of development of vibration diagnostics.
4. To create a more effective technique for controlling, it is necessary to identify a set of controlled parameters of different physical nature as well as to find and justify the relationship between them.

CHAPTER 2. DEVELOPMENT OF A METHOD FOR INTEGRATED CONTROL OF THE TECHNICAL CONDITION OF ELECTROMECHANICAL EQUIPMENT

The tasks of methods and techniques for monitoring the technical condition of sets of traction electro-mechanical equipment (hereinafter referred to as TEE) provide for:

1) determining the object of control at a given time; with regard to TEE, it is preferable to have data on the state of specific units or structural elements of the electrical part and individual motion converters (mechanical part);
2) prediction of one of the future states of these nodes.

The diagnosis of an object is based on a comparison of diagnostic features with their threshold values. In the case of assessing the state of one type of assembly or structural element (for example, a gearbox housing), it is necessary to determine the threshold structural values. When evaluating a TEE which has several types of nodes or structural elements with operating processes of different physical nature, the task of determining the threshold values of a diagnostic feature becomes much more complicated.

2.1. Analysis of signs of defects in the main components of electromechanical equipment

All the main signs of defects and violations of normal motor power conditions are summarized in Table 2.1 [13].

Table 2.1

The Main Defects of Induction Motors

Defect	Low frequency vibration	High frequency vibration	Stator current analysis
Stator winding defects	+	+	+
Rotor winding defects	+	+	+
Static gap eccentricity	+	+	+
Dynamic gap eccentricity	+	+	+
Supply voltage unbalance	+	-	+
Nonlinear voltage distortion	+	+	+

As mentioned in Section 1.1, an object was investigated, which is a typical electromechanical equipment. At JSC "Rīgas elektromašīnbūves rūpnīca", an analysis was made of the malfunctions of the MRM with an asynchronous traction motor (the description of the object is given in Section 5.1) and the external signs of their manifestation (state parameters). The basis for the analysis was the data of the log of acts of work performed, which recorded information about the impacts. The analysis includes data for the period from January 4, 2018 to January 31, 2022.

Despite the listed causes of mechanical failures, most of them are directly related to the electric drive. An analysis of the entire picture of emerging malfunctions of rolling stock electric locomotives showed that it is necessary to introduce control of the condition of mechanical components (wheel sets and traction gearboxes), since these elements are connected with the electric motor by a single energy flow (electrical and mechanical energy) circulating in the drive. The main characteristics of traction MGU are given in Table 5.1.

2.2. Methods for processing diagnostic signals and assessing the technical condition of equipment

Basic provisions for vibration control. Calculation of significant vibration signal frequencies

At present, the frequency spectrum of vibration (vibration velocity, vibration acceleration and vibration displacement) of the assembly is the main input parameter for vibration control. Spectral analysis is based on the selection of the most characteristic and sensitive areas of signal frequencies.

In order to decompose the obtained measurements into the frequency spectrum and identify all the amplitudes of those frequencies at which defects occur, the fast Fourier transformation method (hereinafter referred to as FFT) is used.

Vibration can be divided into three types based on human perceptions: slow motion and visible, invisible but sensible by touching, and insensible by touching but audible as abnormal noise [14]–[24].

Solving the problems of spectral analysis using FFT allows to determine the contribution of individual vibration components to the overall picture of vibration. With the help of FFT, the vibration signal is decomposed into the simplest components of its oscillations of various frequencies and amplitudes [24]. FFT is a method of analysis based on vibration waveform. Generally, waveforms are complicated and difficult to analyse. In FFT, we break waveforms down into a series of discrete sin waves (left chart in Fig. 2.1) and evaluate each individually (right chart in Fig. 2.1).
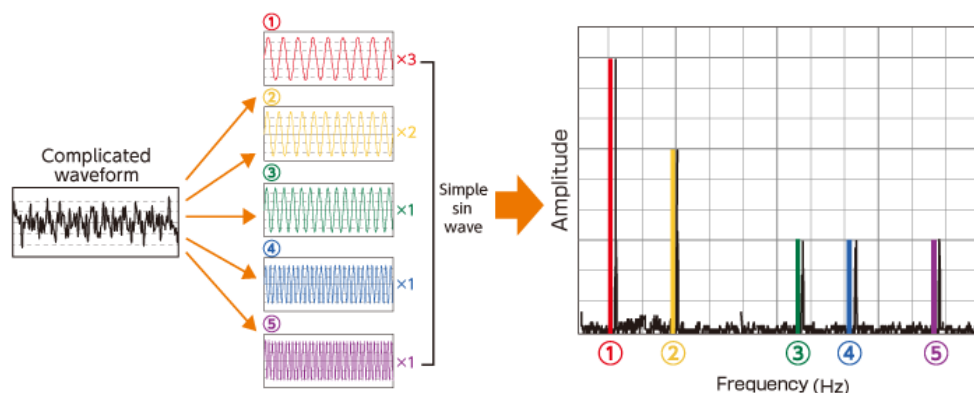
Fig. 2.1. Graphic interpretation of FFT. [18]

The higher the rotational speed of the machine, the higher the vibration frequencies will be, the larger the measured frequency range must be in order to cover vibrations at high frequencies.

For machines consisting of mechanisms that contain toothed gears, blades, finger and gear couplings, rolling bearings, the maximum frequency of the measured frequency range is selected by a 3-fold product, for example, of the number of "blades" (fingers, balls, etc.) on the rotation speed of the machine. The resulting maximum frequency in the calculations (vane, finger, ball, outer and inner ring frequencies) is selected as the maximum frequency of the measured frequency range. Usually, a measurement in such a frequency range makes it possible to obtain all the necessary information about the state of a machine or mechanism [24].

To analyse the obtained spectrum of the vibration signal, it is necessary to know which vibrations and at what frequency occur when a particular defect appears. The most common components in the vibration signal spectrum are the following [24]: reverse frequency, harmonics, subharmonics, resonant frequencies, non-harmonic vibrations, sidebands, and broadband noise.

When recording vibration signals generated by gears, it is necessary to take into account the main characteristic features of their operation described in [3].

The main rule: when gearing defects appear, not only does the amplitude of the gearing harmonic increase, but also side harmonics appear near the gearing frequency.

The frequency shift between the main peak of the gearing harmonic and the side harmonic tells which gear has the suspected defect. If the frequency shift is equal to the reverse frequency of the input shaft, then the defect is located on it, if the shift is equal to the reverse frequency of the output shaft, then the defect is located accordingly. Sometimes there are lateral harmonics from both shafts, while the most defective will be the shaft, the family of lateral harmonics from which will have large amplitudes [25].

The frequencies of manifestation of various defects in gears are the sum of the frequency of gearing (F_z) as well as the rotational frequencies of the input and output shafts (F_{r1} and F_{r2}).

The gearing frequency F_z is found by formula [3]

$$F_z = Fr_n z_n, \qquad (2.1)$$

where z_n is the largest number of teeth in a tooth pair and Fr_n is rotational frequency of the wheel with the largest number of teeth, Hz.

The harmonic amplitude at the gear frequency is usually very sensitive to load. When analysing the spectra of vibration signals, the most serious attention should be paid to [3]:
- the presence in the vibration spectrum near the gearing harmonic of lateral harmonics from the main gearing frequency, located to the left and right, in frequency, from the F_z peak;
- the relative magnitude of the amplitude of these lateral harmonics of the gearing frequency in relation to the amplitude of the peak of the main gearing frequency;
- the value of the frequency step of alternation of the lateral harmonics of the toothing frequency: how much they are shifted relative to each other and relative to the main harmonic;

- the presence in the spectrum of a characteristic hump (humps) of "white noise" near the gearing frequency, its average level relative to the harmonic of the gearing frequency itself, and the relative power level concentrated in each hump;
- the presence of peaks and "white noise" in the spectrum in all other frequency bands of the vibration spectrum, located in areas that at first glance are not related to the gearing frequency.

Table 2.2 presents gear defects and their frequency values [26].

<div align="right">Table 2.2</div>

Frequency of Occurrence of Defects in Gear Transmission

Gear defect	Fundamental defect frequency	Harmonics	Development of a defect
Gear pair wear (defect on the input shaft)	$F_z,\ F_z \pm k \cdot F_{r1}$	3 side harmonics, unpaired	"White noise"
Gear pair wear (output shaft defect)	$F_z,\ F_z \pm k \cdot F_{r2}$	+ (4–5 side harmonics)	"White noise"
Gear eccentricity	$F_z \pm k \cdot F_{r1}$ or $F_z \pm k \cdot F_{r2}$	$k = 1,2,3,4,5,...$	Side harmonics rise
Gear misalignment	$k \cdot F_z$	$k = 1,2,3$	The appearance of side harmonics
Cracked (broken) tooth	Timing signal analysis	–	On the oscillogram, it is possible to track the amplitude of the beats

The maximal frequency of the received signal for controlled gears can be quite high. For the object under study, with the maximum number of revolutions – 4653, the frequency value reaches 1.94 kHz for the first and most loaded gear stage ($z = 25$) and 860.1 Hz for output stage ($z = 61$).

2.3. Main results and conclusions of Chapter 2

Depending on the type and form of the diagnostic experiment, there are test, functional and functional-test diagnostic systems. In test diagnostic systems, the impact on the diagnosed object comes from the diagnostic tools. In systems of functional diagnostics, the impacts coming to the diagnosed object are set by the working algorithm of functioning.

According to the type of vibration signal acquisition, systems with parallel and serial measurement are distinguished.

As practice shows, it is not advisable to reduce the number of measuring points, and, consequently, the number of vibration sensors [27], since there is no strongly pronounced correlation between different measuring points.

It is possible to increase the reliability of diagnosis by reducing instrumental, methodological and subjective errors. It is possible to reduce the instrumental error by using measuring equipment with higher metrological characteristics in the vibration diagnostics system. It is possible to reduce the methodological error by using more advanced algorithms and diagnostic technology. To eliminate subjective error (human factor), it is necessary to completely exclude the influence of the operator on the diagnosis.

CHAPTER 3. INVESTIGATION OF THE STATIC STRENGTH OF THE TRACTION GEAR IN THE MOTOR BOGIE COMPOSITION

3.1. Development of a model of an electromechanical drive system

The operation of the traction gearbox drive almost all the time occurs in dynamic modes. Intensive conversion of electrical energy into mechanical energy on the motor shaft, transfer of kinetic energy in the elements of the gearbox and in the elastic system of the gearbox-wheel pair determines the continuity of the loads. The magnitude of dynamic loads that occur in the elements of the MGU depends on the energy and kinematic characteristics of the drive: motor power, drive speed and acceleration, inertia of rotational units, and external influences, including shock loads on the wheelset.

To study the influence of external conditions and drive characteristics (kinematic and energy) on the load of the gearbox elements, it is necessary to develop a traction drive model, which is a single electromechanical system in which the electrical and mechanical parts in the dynamic modes of operation of the mechanism are in continuous interaction.

3.2. Study of the static strength of the gearbox elements

The power electrical circuit of the motor coach of the suburban electric train is shown in Fig. 3.1. Each motor car (train lineup of 11 cars has 5 motor cars) has two motor bogies, each of which contains two MGU controlled by a traction converter.
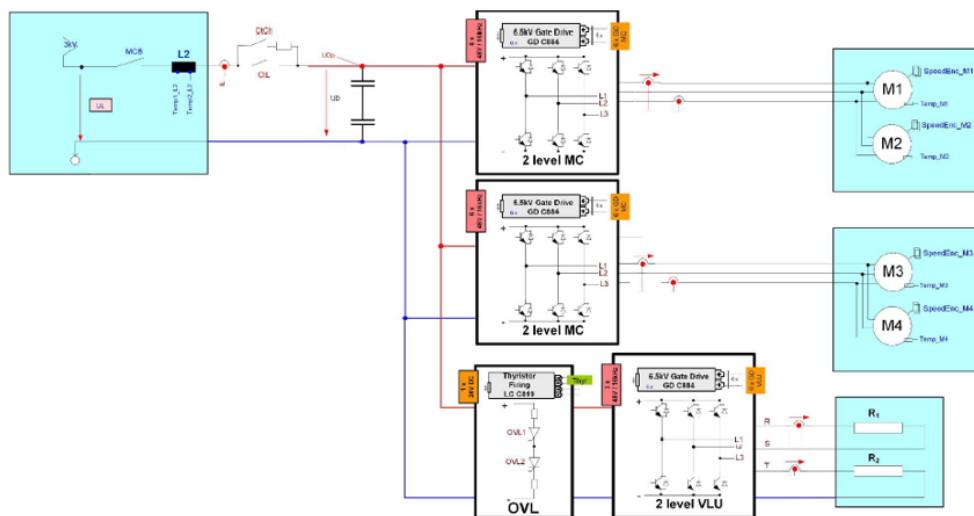
Fig. 3.1. Control scheme of traction MGU by means of inverters [28].

L2 – input line choke; 2 level MC – two-level converter on IGBT transistors; OVL and 2 level VLU – braking control system on power thyristor; M1 and M2 – traction MGU of motor bogie No. 1; M3 and M4 – traction MGU of motor bogie No. 2; R1 and R2 – braking resistors.

The power section is a system of two MGUs with asynchronous motors functionally made according to the "generator-motor" structure with twin control by means of a converter on IGBT transistors. The block diagram of the electrical part of the electromechanical system, created in the MATLAB Simulink program, is shown in Fig. 3.2 [28].
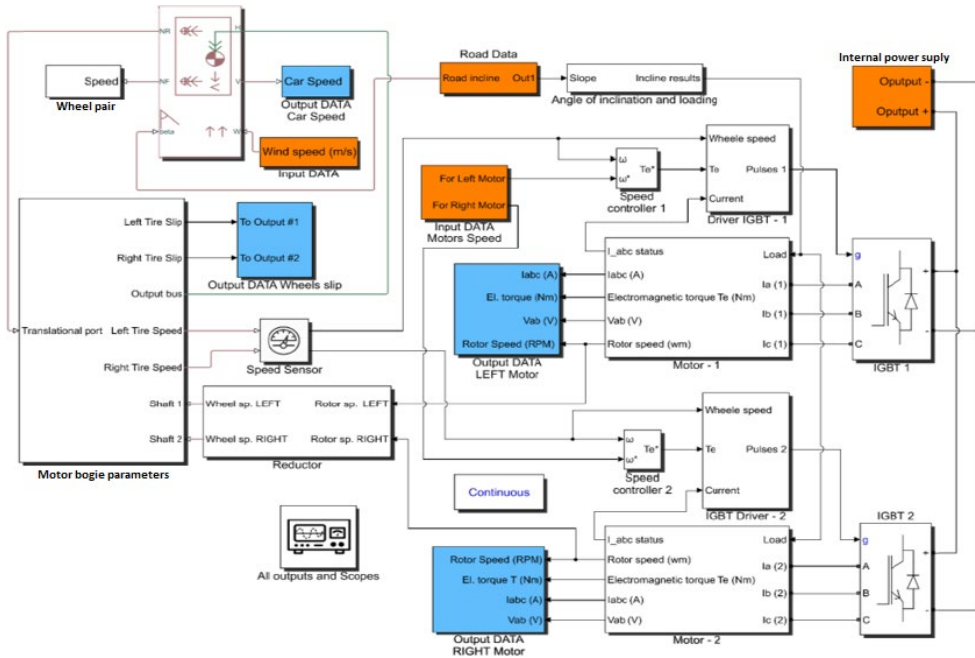
Fig. 3.2. Implementation of the researched TL mathematical model in MATLAB Simulink.

The reference signal U_{input} is fed to the speed controller VR, from which the error signal is fed to the current controller IR through the IMAX limiting block (current cutoff). The current regulator IR gives a reference signal to the voltage regulator UR, the output from which goes to the IGBT converter that feeds the winding of the loaded motor (RIGHT Motor), which, by controlling the current in the winding, determines the set voltage level. Next, the voltage is applied to the load motor (LEFT Motor), which is represented by an aperiodic link with EMF feedback. Feedback signals proportional to speed, current and voltage via sensors V_S, I_S and U_S are fed to their respective regulators [28]–[32].

The obtained parameters of the transient process of reaching the nominal parameters for a mutually loaded pair of MGU shown in Fig. 3.3, and traction – power energy characteristics of the drive shown in Fig. 3.4 and EMU output torque cyclogram in Fig. 3.5.

The preliminary verification of the model was carried out in two stages. Stage 1: starting the motor at a speed of 0.5 ω_{nom} with a load moment $M_c = 0.3\ M_{nom}$ and locking the drive with $M_{stop} = 2M_{nom}$. The maximum M_{d_max} and integral $\int M_d$ values of the moments of the motors M_d, the gear shafts $S_2\ M_{s-g} = M_{12}$ and on the wheelsets $M_w = M_{23}$ were registered.

Stage 2: starting the motor at a speed of 0.5 ω_{nom} with a load moment $M_c = M_{nom}$ and stopping with $M_{stop} = 2\ M_{nom}$.

The results of a preliminary check of the operability of the circuit in the modes of starting and stopping with different loads showed:

- in the start mode with $M_c = 0.3\,M_{nom}$, the load on the motor is the largest in terms of integral and maximum values, their minimum values are on the output shaft;
- when starting with $M_c = M_{nom}$, the load on the motor is the largest, the minimum value is on the gear shaft S_2;
- the loads that occur on the gear shaft S_2 and on the shaft of the wheelset in start-up modes with $M_c = 0.3\,M_{nom}$ and $M_c = M_{nom}$ are comparable and practically do not differ;
- integral indicators of the load moment on the gear shaft S_2 in the locking mode are 15–30 % higher compared to the motor and depend on the load moment on the output shaft of the wheelset;
- the integral load on the gear shaft S_2 is less than on the output shaft of the wheelset, the difference is 7 %, the value of the maximum load on the gear shaft S_2 is less than on the output shaft by 3 %.

Oscillograms of the speed, current and torques of the motor, gear shaft in the start mode for Stage 1 and Stage 2 of simulation are shown in Figs. 3.6 and 3.7.
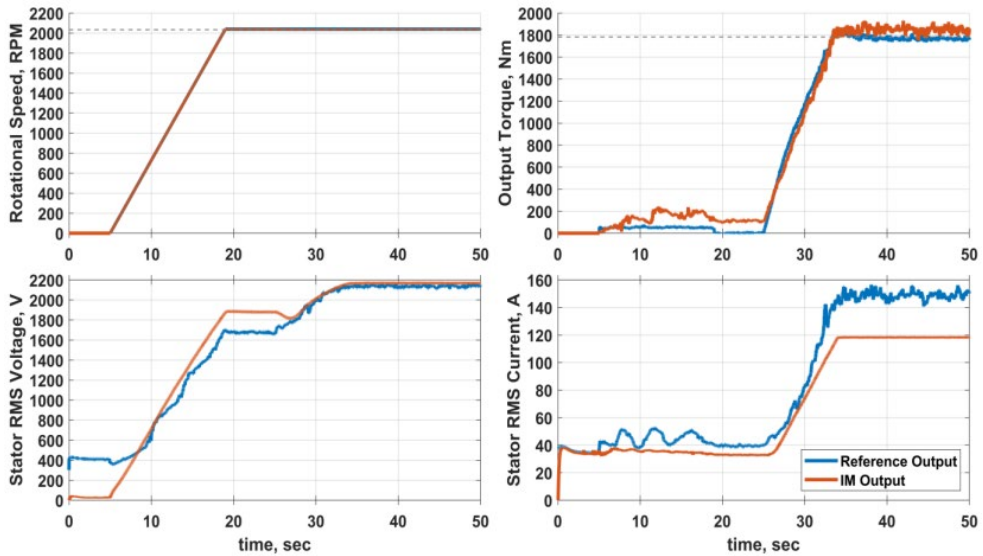
Fig. 3.3. Transient process reaching the nominal parameters for a mutually loaded MGU.
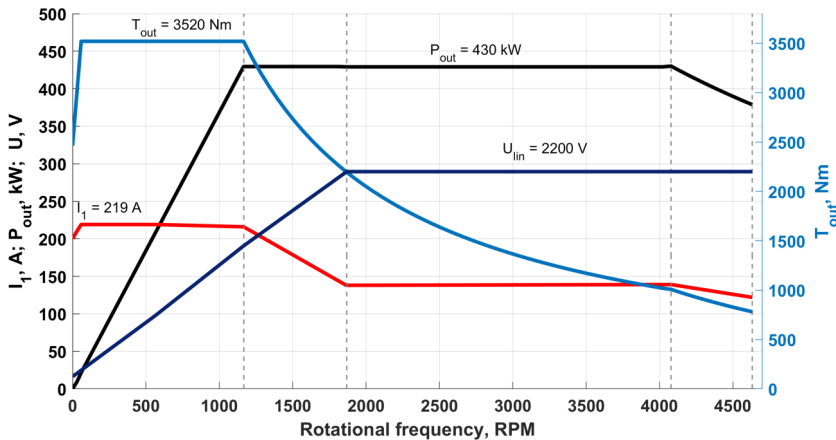
Fig. 3.4. Traction power energy characteristics of the drive.

19
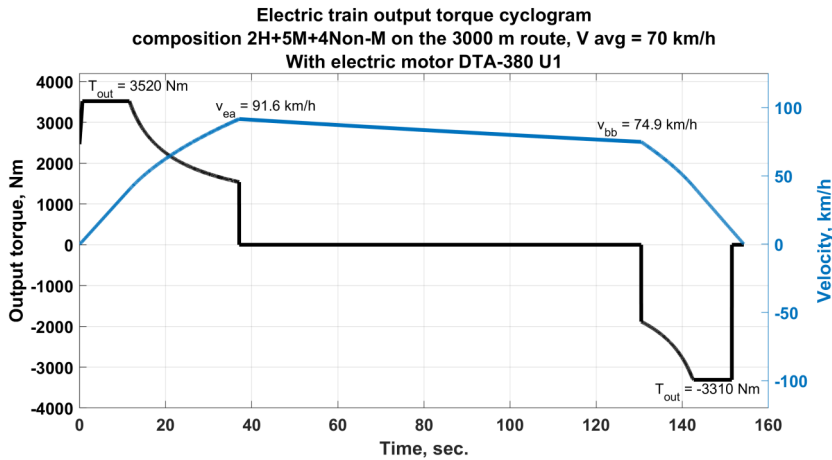
Fig. 3.5. EMU output torque cyclogram with 380 kW MGU.

3.3. Calculation of stresses of the MGU structure

Determination of the physical conditions of simulation. The conducted studies of the loading of the gearbox elements, performed on the electromechanical model of the MGU drive, made it possible to establish the maximum loads that occur on the housing in dynamic modes. In this regard, it is necessary and sufficient to calculate the stress-strain state in a static loading model. For this purpose, the FEMAP static strength analysis is used. The model uses the following coordinate system:

X – longitudinal axis (positive to the left);

Y– transverse axis;

Z – vertical axis.

The next step is to set the properties of the material. The body is made of structural ductile iron EN-GJS-350-22-LT with the following strength properties [33]:

- modulus of elasticity $E = 169\ 000$ MPa;
- Poisson's ratio $\mu = 0.275$;
- yield strength $\sigma_y = 220$ MPa.

The resulting model for analysing the stress-strain state of the hull is shown in Fig. 3.6.
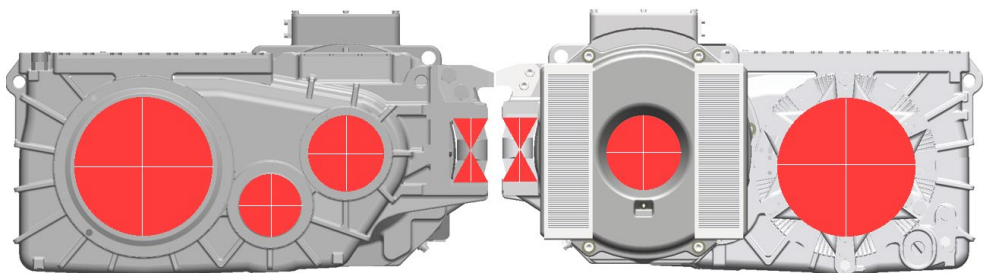
Fig. 3.6. Mesh of the finite element model of the hull.

As a result of the performed calculations with further analysis of the results it was possible to establish that the seating surface is a place of significant stress concentration.

The forces generated in the gearing cause reaction forces in the bearings according to the data presented in Table 3.1.

Table 3.1

Initial Model Data

Parameter	Designation	Meaning
Traction motor shaft power in continuous mode (kW)	P_N	380
Maximum starting torque of the traction motor (Nm)	M_{max}	3 551
Rated drive motor starting torque (Nm)	M_N	1 176
Maximum clutch slip torque (Nm)	M_S	11 000
Traction motor rotor speed, maximal constructive value (min^{-1})	n	4 774
Place of application of the acceleration	Direction of acceleration	Acceleration values, g
Acceleration on gear housing and traction motor for strength (g)	Vertical	15
	transverse	15
	longitudinal	15
Acceleration on gearbox housing and traction motor for fatigue (g)	Vertical	5.4
	transverse	4.7
	longitudinal	2.5

The model contains a gearbox housing and a traction motor housing. The electrical part of the stator is replaced by a weight at the centre of gravity, as shown in Fig. 3.7. Traction silent blocks are replaced by a spring element. Finite element sizes vary from 6 to 12 mm. The model includes 773 125 elements and 1 296 304 nodes. The structure is modelled by finite elements of the types like "TETRA 10" and "Springs" [33].
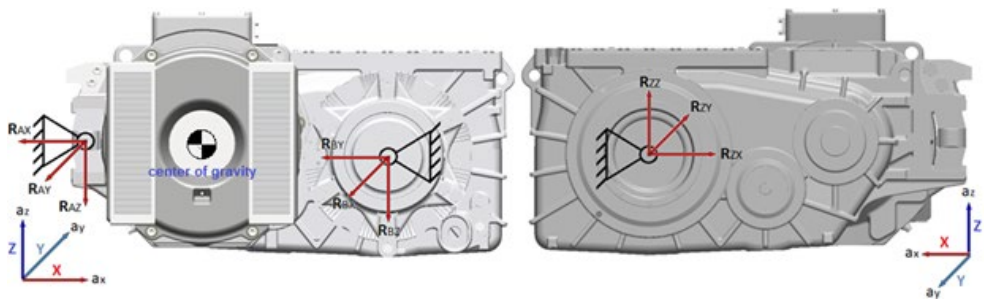
Fig. 3.7. Fixing scheme for load modes I, II, III.

Determination of the static strength of the MGU structure in the Thesis is proposed to be carried out in 3 modes with forward and reverse directions of rotation for each mode.

Mode I (forward direction of rotation)

Mode I is calculated for the maximum motor torque when starting from a standstill of 3551 Nm. The torque is transferred to the gear in the form of forces:

tangential force $F_t = 2\,M_{rot}/D_0 = 49\,891$ N;

radial force $F_r = F_t \cdot tg\alpha / cos\beta = 18\,800$ N, where $\alpha = 20°$, $\beta = 15°$;

axial force $F_a = F_t \cdot tg\beta = 13\,368$ N, where $\beta = 15°$ (forces explication and graphic discription of D_0 see in APPENDICES I and II).

Table 3.2 shows the load values in the 1st, 2nd and 3rd gear bearings in the coordinate system.

Load in Bearings of the 1st, 2nd and 3rd stage in the Coordinate System

Bearing No.	Force [N]							
	x′		y′		z′		xz′	
Direction	forward direction of rotation	reverse direction of rotation	forward direction of rotation/reverse direction of rotation	forward direction of rotation	reverse direction of rotation	forward direction of rotation	reverse direction of rotation
1st stage								
B1	11 876	−27 763	0	20 301	−15 391	23 478	31 746
B2	−31	−14 993	0	29 979	−18 283	29 973	23 649
B3	0	0	13 389 / −13 389	0	0	0	0
2nd stage								
B4	7 847	−41 149	−21 060 / −21 878	−77 050	57 861	77 436	70 982
B5	−27 093	27 361	28 832 / 19 017	−65 999	44 047	71 276	51 853
3rd stage								
B6	0	0	−31 293 / −21 078	0	0	0	0
B7	0	0	10 154 / 42 221	0	0	0	0

Further, the mode includes impacts in all directions of X, Y and Z coordinates with accelerations: $a_x = \pm 15$ g; $a_y = \pm 15$ g; $a_z = \pm 15$ g.

Mode I (forward and reverse rotation)

Figure 3.8 shows the resulting radial, axial loads, as well as the inertial radial loading of bearings and the reaction of the accelerating force in the labyrinths for simulated Mode I for forward rotation.
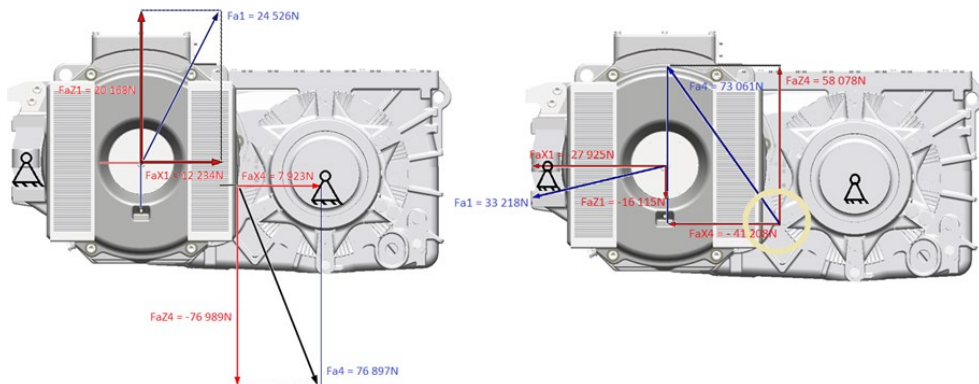
Fig. 3.8. Radial load of the 1st and 4th bearing in simulated Mode I.

Mode II (forward and reverse rotation)

Mode II is calculated for a maximum starting torque of 11 000 Nm. The torque is transferred to the gear in the form of forces [33]:
- tangential force $F_t = 2M_{rot}/D_0 = 154\ 549$ N;
- radial force $F_r = F_t \cdot tg\alpha / \cos\beta = 58\ 235$ N, where $\alpha = 20°$, $\beta = 15°$;
- axial force $F_a = F_t \cdot tg\beta = 41\ 411$ N, where $\beta = 15°$.

Table 3.3 shows the load values in the 1st, 2nd and 3rd stage bearings in the coordinate system.

Table 3.3

Load in Bearings of the 1st, 2nd and 3rd stage in the Coordinate System

Bearing No.	Force [N]							
	x'		y'	z'		xz'		
Direction	forward direction of rotation	reverse direction of rotation	forward direction of rotation/reverse direction of rotation	forward direction of rotation	reverse direction of rotation	forward direction of rotation	reverse direction of rotation	
1st stage								
B1	36 731	−86 102	0	68 531	−41 931	77 734	95 667	
B2	−103	−46 513	0	90 793	−58 612	90 799	74 795	
B3	0	0	41 439 / −41 439	0	0	0	0	
2nd stage								
B4	24 317	−127 397	−65 054 / −67 979	−238 039	179 967	239 278	220 473	
B5	−283 376	84 743	89 145 / 43 867	−203 534	137 399	219 931	161 436	
3rd stage								
B6	0	0	−97 101 / −65 073	0	0	0	0	
B7	0	0	31 673 / 131 117	0	0	0	0	

Figure 3.9 shows the resulting radial, axial loads, as well as the inertial radial loading of bearings and the reactions of the accelerating force in the labyrinths for calculated Mode II.
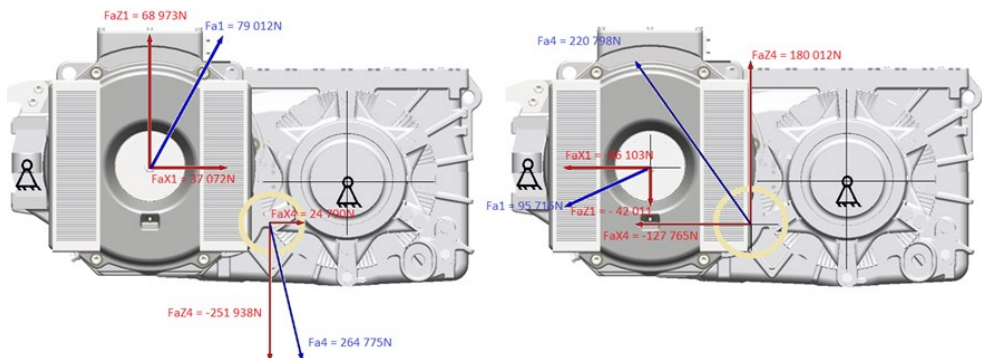
Fig. 3.9. Radial load of the 1st and 4th bearing in calculated Mode II.

Mode III (forward and reverse rotation)

Mode III is calculated for motor torque up to 1176 Nm and impacts. The magnitude of the forces arising in the gearing are equal to [33]:

tangential force $F_t = 2M_{rot} / D_0 = 24\,953$ N;

radial force $F_r = F_t \cdot tg\alpha / \cos\beta = 9\,402$ N, where $\alpha = 20°$, $\beta = 15°$;

axial force $F_a = F_t \cdot tg\beta = 6686$ N, where $\beta = 15°$.

Further, shocks in all directions of coordinates with accelerations are included in Mode III:

$a_x = \pm 2.5$ g (longitudinal impact);

$a_y = \pm 4.7$ g (axial impact);

$a_z = \pm 5.4$ g (impact in the vertical direction).

Further, in Table 3.4, the load values in bearings of the 1st, 2nd and 3rd stage are given in the coordinate system.

Table 3.4

Load in Bearings of the 1st Stage in the Coordinate System

Bearing No.	Force [N]							
	x′		y′	z′		xz′		
Direction	forward direction of rotation	reverse direction of rotation	forward direction of rotation/reverse direction of rotation	forward direction of rotation	reverse direction of rotation	forward direction of rotation	reverse direction of rotation	
1st stage								
B1	6 103	−14 179	0	9 102	−9 143	10 757	16 701	
B2	−102	−7 573	0	15 997	−8 759	15 625	11 687	
B3	0	0	6 902 / −6 902	0	0	0	0	
2nd stage								
B4	4 079	−20 876	−10 729 / − 10 998	−38 943	28 876	39 046	35 514	
B5	−13 543	13 734	14 703 / 7 103	−33 477	21 918	35 984	26 001	
3rd stage								
B6	0	0	−16 901 / −11 002	0	0	0	0	
B7	0	0	32 137 / 21 993	0	0	0	0	

Figure 3.10 shows the resulting radial, axial loads, as well as the inertial radial loading of bearings and the reactions of the accelerating force in the labyrinths for simulated Mode III.
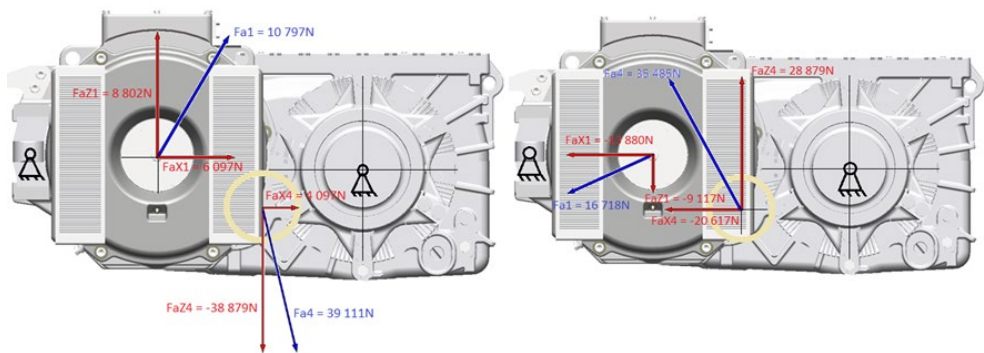
Fig. 3.10. Radial load of the 1st and 4th bearing in simulated Mode III.

3.4. Main results and conclusions of Chapter 3

1. A traction drive model has been developed, which is a single electromechanical system in which the electrical and mechanical parts in dynamic modes are in continuous interaction.

2. The developed model allows to study the maximum and integral load indicators on the most loaded transmission elements – gear shafts: primary shaft i_1: $z = 25$, $m = 5.5$; intermediate shaft i_2: $z = 26$, $m = 7$; i_3: $z = 56$, $m = 5.5$; and output shaft i_4: $z = 61$, $m = 7$.

3. During the simulation, it was found that the value of the integral load on the gear shaft $z = 61$, $m = 7$ is less than on the primary stage by 24.7 %. Primary shaft $z = 25$, $m = 5.5$ is the most loaded element in the drive gearbox.

4. A finite element model of the gearbox housing at the points of rotation of the gear shaft has been developed. The places of maximum loads are found, the calculation of stresses is carried out taking into account the maximum values. The maximum stresses are concentrated in the seating area of the 7th bearing. The reliability of the model is confirmed by an analytical solution.

CHAPTER 4. INFLUENCE OF LOADS ON THE RESOURCE OF THE GEAR BEARING ELEMENTS

4.1. Evaluation of the safety margin of the gear housing according to the allowable stresses

The operation of the drive mainly consists of two modes: acceleration and deceleration. The loads that occur on the elements of the gearbox in these modes determine the intensity of their wear. In this regard, it is necessary to know the magnitude of the stresses that appear on the elements of the gearbox when the specified loads are applied and the ability of the housing to resist destruction. Further, it is considered how the loads on the hull change under various modes of operation of the MGU, the end of which will be the locking of the wheelset. In the analysis, we will use the developed drive model and the finite element model of the housing.

The calculations of stresses on the fillet of the gear shaft showed that their values vary from 6686 N to 41411 N and depend on the operating modes of the mechanism. To assess the degree of influence of loads on the resource of the housing, it is necessary to determine the ability of the element to resist fatigue failure at different levels in the mechanism.

The assessment of safety margin or allowable stresses is carried out by calculation for the cases of the most unfavourable possible combination of simultaneously acting standard loads in accordance with the design modes [33]. The total stresses obtained as a result of the calculation should not exceed the allowable values presented in Table 4.1 for the corresponding simulated modes (σ_y – conditional material yield strength EN-GJS-350-22-LT according to EN 1563-2011).

Table 4.1

Permissible Stresses for the Housing of Gearbox Elements

Simulated Mode	Permissible stress for constructive elements
Mode I	0.9 σ_y
Mode II	0.9 σ_y
Mode III	0.9 σ_y

The gearbox housing equivalent stress values in Modes I and II are shown in Figs. 4.1 and 4.2. Data and calculated safety factor for Mode I are presented in Tables 4.2, 4.3 and 4.4 [33].

Table 4.2

Equivalent Stresses and Safety Margin for Mode I. Forward Rotation

σ_{eq}		σ_y	0.9 σ_y	Safety margin 0.9 σ_y/σ_{eq}
(15; 15; 15) g	137.0	220	198	1.445
(−15; −15; −15) g	132.4	220	198	1.495
(−15; −15; 15) g	134.7	220	198	1.470
(−15; 15; 15) g	133.9	220	198	1.479
(15; −15; 15) g	139.9	220	198	1.415
(15; 15; −15) g	134.9	220	198	1.468
(15; −15; −15) g	138.3	220	198	1.432
(−15; 15; −15) g	132.2	220	198	1.498

The minimal value of safety margin $n = 0.1$ for Mode I.

Forward rotation

(15; 15; 15) g

(−15; −15; −15) g

Reverse rotation
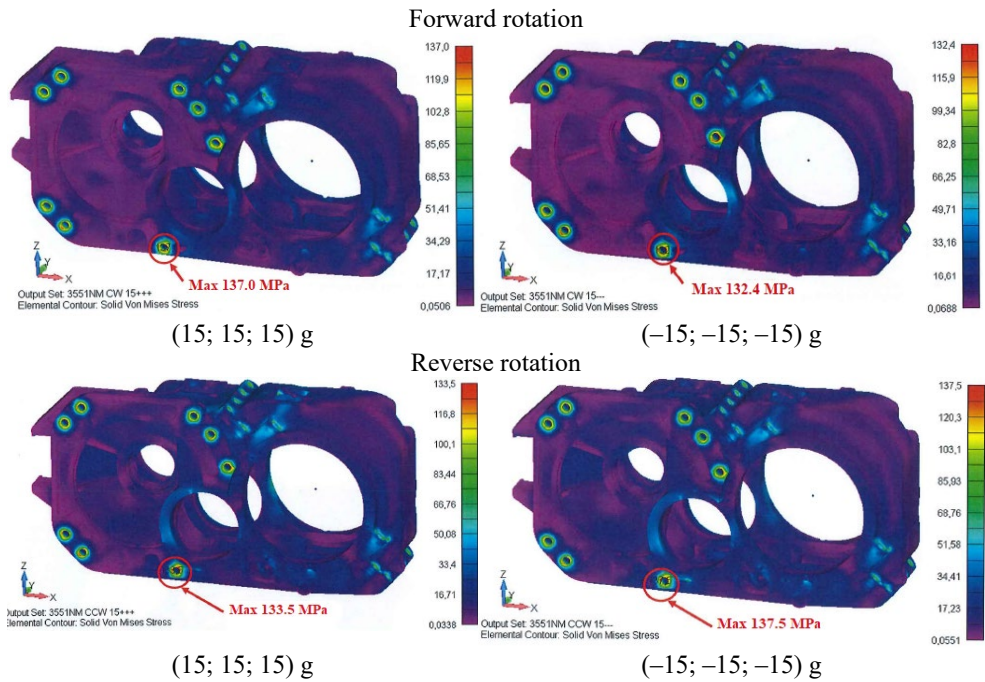
(15; 15; 15) g

(−15; −15; −15) g

Fig. 4.1. Equivalent housing stresses in Mode I for forward and reverse rotation.

Table 4.3

Equivalent Stresses and Safety Factor for Mode I
Reverse Rotation. The Minimal Value of Safety Margin $n = 0.1$ for Mode I

σ_{eq}		σ_Y	0.9 σ_Y	Safety margin 0.9 σ_Y/σ_{eq}
(15; 15; 15) g	133.5	220	198	1.483
(−15; −15; −15) g	137.5	220	198	1.440
(−15; −15; 15) g	137.7	220	198	1.438
(−15; 15; 15) g	141.3	220	198	1.401
(15; −15; 15) g	135.9	220	198	1.457
(15; 15; −15) g	134.2	220	198	1.475
(15; −15; −15) g	137.1	220	198	1.444
(−15; 15; −15) g	138.1	220	198	1.434
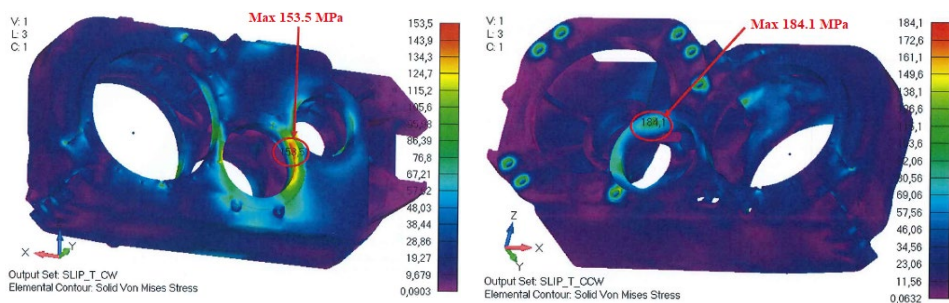
Fig. 4.2. Equivalent housing stresses in Mode II for forward rotation.

Table 4.4

Equivalent Stresses and Safety Margin Values for Mode II

σ_{eq}		σ_y	0.9 σ_y	Safety factor 0.9 σ_y/σ_{eq}
Forward rotation	153.5	220	198	1.291
Reverse rotation	184.1	220	198	1.083

The minimal value of safety factor $n = 0.1$ for Mode II.

4.2. Evaluation of structural fatigue resistance

The assessment of the fatigue resistance of load-bearing elements is made depending on the available information regarding the loading of the element and the parameters of the material fatigue curve. Further, Fig. 4.3 shows the main maximum forces of the gearbox housing in Mode III for the forward direction [33].
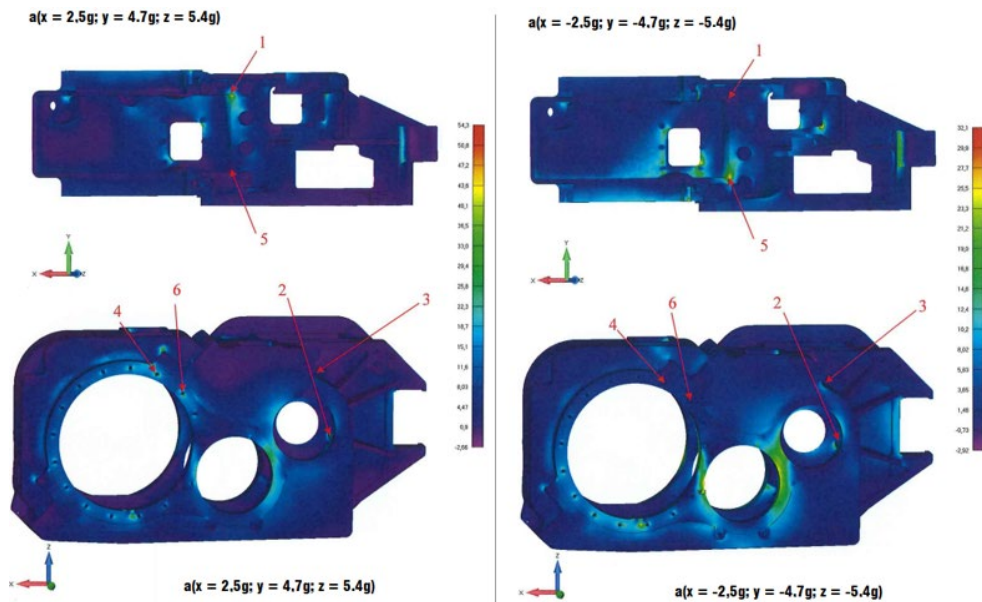
Fig. 4.3. Maximal gear housing forces in Mode III.

The values for the fatigue safety margins for the forward direction are given in Table 4.5.

Table 4.5

Calculated Values of the Fatigue Resistance Safety Margin. Direct Rotation

Indicator	Values					
Stress point No. (max)	1	2	3	4	5	6
σ_{max}	55.9	75.2	49.9	41.8	35.8	42.1
σ_{min}	−3.8	18.1	3.4	1.1	−3.3	4.9
$\sigma_m = (\sigma_{max} + \sigma_{min})/2$	26.05	46.65	26.65	21.45	16.25	23.5
$\sigma_a = \sigma_{max} - \sigma_m$	29.85	28.55	23.25	20.35	19.55	18.60
ψ_σ	0.3	0.3	0.3	0.3	0.3	0.3
α_σ	1	1	1	1	1	1
K_σ	1.83	1.83	1.83	1.83	1.83	1.83
n	2.55	2.41	2.85	3.64	3.95	3.87

Figure 4.4 shows the main maximum forces of the gearbox housing in Mode III for the reverse direction of rotation [33].
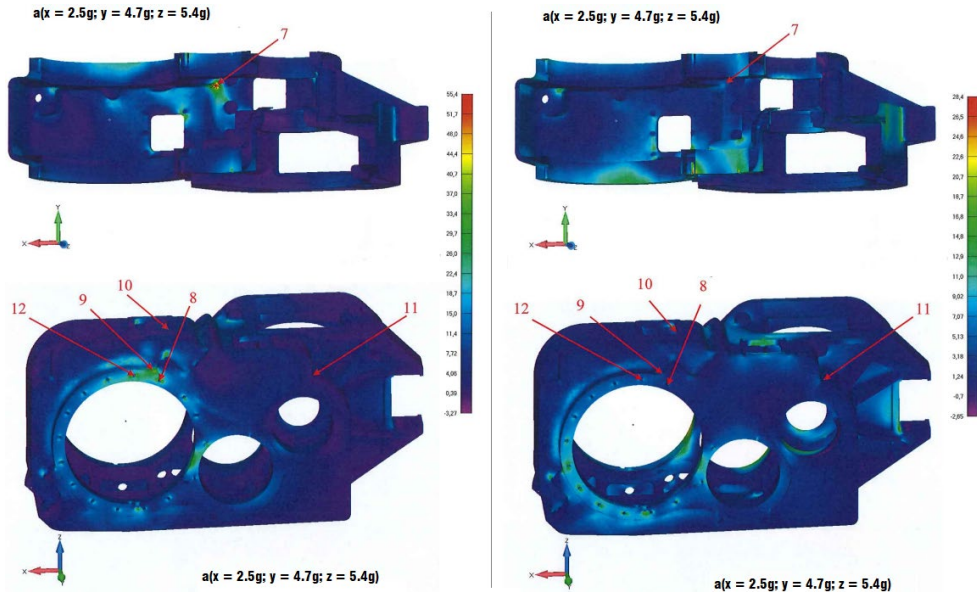
Fig. 4.4. Maximum main stresses of the gearbox housing in Mode III for reverse direction.

The calculated values for the fatigue safety margins for the forward direction of rotation are given in Table 4.6.

Calculated Values of the Fatigue Resistance Safety Margin. Direct rotation

Indicator	Values					
Stress point No. (MAX)	7	8	9	10	11	12
σ_{max}	80.9	55.1	54.6	46.7	41.1	54.6
σ_{min}	11.0	6.7	6.8	−0.3	−5.3	11.6
$\sigma_m = (\sigma_{max} + \sigma_{min})/2$	45.95	30.9	30.7	23.2	17.9	33.1
$\sigma_a = \sigma_{max} - \sigma_m$	34.95	24.2	23.9	23.5	23.2	21.5
ψ_σ	0.3	0.3	0.3	0.3	0.3	0.3
α_σ	1	1	1	1	1	1
K_σ	1.82	1.82	1.82	1.82	1.82	1.82
n	2.05	2.97	3.01	3.24	3.37	3.25

4.3. Main results and conclusions of Chapter 4

For working Mode I, the minimal allowable margin of safety in the calculation of strength for allowable stresses is $[n] > 1.0$. Data on simulated modes are summarized in Table 4.7.

To calculate the strength for allowable stresses, the minimum calculated margin of safety is $n = 1.40$, which is more than the minimal allowable value. The design of the gearbox housing complies with the requirements of GOST R 55513. For calculated Mode III, according to the assessment of the fatigue resistance of load-bearing elements, the minimal allowable margin of

safety is $[n] > 2.0$. Data of calculated points for fatigue assessment are summarized in Table 4.8.

Table 4.7

Values of Safety Margin for Allowable Stresses

Simulated mode	n_{min} (calculated)	$[n]$	Safety margin for the selected construction
Mode I (forward rotation)			
(15; 15; 15) g	1	1.445	sufficient
(−15; −15; −15) g	1	1.595	sufficient
(−15; −15; 15) g	1	1.47	sufficient
(−15; 15; 15) g	1	1.479	sufficient
(15; −15; 15) g	1	1.415	sufficient
(15; 15; −15) g	1	1.468	sufficient
(15; −15; −15) g	1	1.432	sufficient
(−15; 15; −15) g	1	1.98	sufficient
11 000 Nm	1	1.291	sufficient
Mode I (reverse rotation)			
(15; 15; 15) g	1	1.483	sufficient
(−15; −15; −15) g	1	1.44	sufficient
(−15; −15; 15) g	1	1.438	sufficient
(−15; 15; 15) g	1	1.401	sufficient
(15; −15; 15) g	1	1.457	sufficient
(15; 15; −15) g	1	1.475	sufficient
(15; −15; −15) g	1	1.444	sufficient
(−15; 15; −15) g	1	1.434	sufficient
11 000 Nm	1	1.083	sufficient

Table 4.8

Values of Safety Margin for Allowable Stresses

Simulated mode	n_{min} (calculated)	$[n]$	Safety margin for the selected construction
Mode III (forward rotation)			
1	2	2.55	sufficient
2	2	2.41	sufficient
3	2	2.85	sufficient
4	2	3.64	sufficient
5	2	3.95	sufficient
6	2	3.87	sufficient
Mode III (reverse rotation)			
7	2	2.05	sufficient
8	2	2.97	sufficient
9	2	3.01	sufficient
10	2	3.24	sufficient
11	2	3.37	sufficient
12	2	3.25	sufficient

For the remaining calculated points of fatigue strength, the minimum margin of safety is higher than the minimum allowable coefficient when assessing fatigue resistance, which corresponds to the fatigue requirements in accordance with norms.

CHAPTER 5. DETERMINATION OF THE LEVEL OF VIBROACTIVITY OF THE TRACTION MGU CONSIDERING THE INTERRELATIONS WITH THE DRIVE ARCHITECTURE

5.1. Determination of the traction drive model parameters

For the normal operation of the rolling stock, it is necessary that the resonant frequencies appear, at best, beyond the operating speed range, or at speeds below 60 km/h. So, with some residual imbalance of the motor rotor for a train speed of 120 km h (corresponding to 155 Hz), resonant oscillations of the MGU will appear, which is unacceptable. In order to shift the resonance to the region of speeds less than 60 km/h, it is necessary that the natural frequency of the MGU and the bogie be less than 50 Hz. To analyse vibration disturbances from the side of the MGU, an analysis of the equations of oscillations of the "bogie frame – MGU" system was carried out to determine the equivalent method of fixing the MGU on a vibration test bench. Under these conditions, the MGU oscillations along the X, Y, Z coordinates will be independent when the coordinates of the MGU fixing points change.

The traction motor parameters for entering them into the MATLAB/Simulink model for checking the natural vibration of an **uncoupled and unloaded MGU** are presented in Table 5.1, and the characteristics of the motor for idle running are shown in Fig. 5.1.

Table 5.1

Typical No-load MGU Characteristics at 155.1 Hz

U_0	I_{0_min}	I_{0_max}	P_{0_min}	P_{0_max}	$cos\varphi_{min}$	$cos\varphi_{max}$
V	A	A	kW	kW	r.u.	r.u.
2280	27.6	34.1	11.7	14.4	0.096	0.119
2200	26.0	32.2	11.2	13.8	0.101	0.125
2020	22.6	27.9	9.8	12.1	0.111	0.137
1725	17.4	21.5	7.8	9.6	0.135	0.166
1525	14.3	17.7	6.7	8.3	0.159	0.196
1425	12.9	16.0	6.2	7.7	0.173	0.214
1225	10.4	12.8	5.4	6.6	0.216	0.267
1025	8.3	10.2	4.6	5.6	0.282	0.348
725	5.9	7.2	3.8	4.7	0.461	0.569
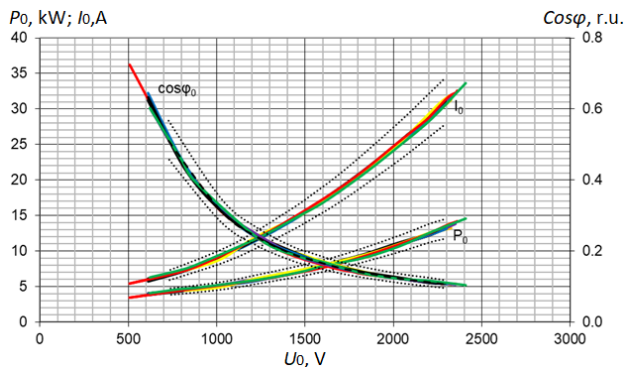
Fig. 5.1. Typical no-load MGU characteristics at 155.1 Hz.

The motor parameters for entering into the MATLAB/Simulink model for checking vibration in the **mutual load mode for coupled and mutually loaded MGU** are presented in Table 5.2, and the motor characteristics for the traction mode are shown in Fig. 5.2.

Typical Operating MGU Characteristics at 155.1 Hz

M	I_{min}	I_{max}	$cos\phi_{min}$	$cos\phi_{max}$	s_{min}	s_{max}	η_{min}	η_{max}
Nm	A	A	r.u.	r.u.	%	%	%	%
217	32.3	39.8	0.767	0.947	0.20	0.27	87.1	95.5
318	44.4	54.8	0.795	0.982	0.30	0.41	89.3	98.0
418	57.3	70.7	0.802	0.990	0.40	0.53	89.9	98.6
520	71.0	87.7	0.798	0.985	0.54	0.67	90.2	99.0
622	85.7	105	0.788	0.972	0.65	0.80	90.3	99.0
726	102	126	0.769	0.950	0.80	0.99	89.9	98.5
831	122	150	0.739	0.913	0.99	1.23	89.4	98.0
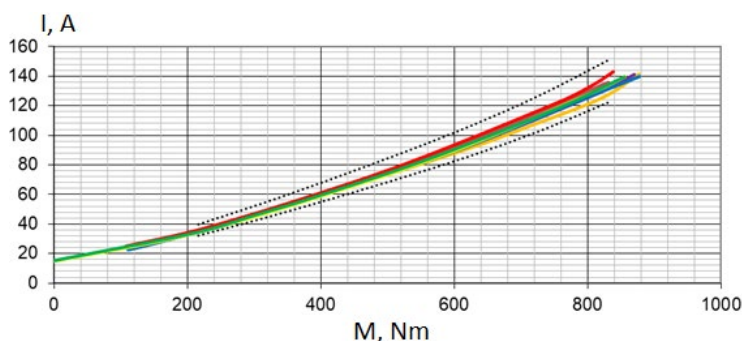
Fig. 5.2. Typical operating characteristics at 155.1 Hz.

The study of the amplitude-frequency characteristics of the MGU vibration has been carried out. The developed technique is intended for use at the vibration characteristics research stand. Based on the measurements obtained, an analysis of the results was made, which showed the presence of electromechanical resonance and the rotor imbalance.

By its purpose, the MGU is connected to a converter, which inherently is a powerful source of harmonics with smooth regulation of the supply voltage of traction motors in the traction mode and smooth regulation of the inverter back EMF in the regenerative braking mode.

The test at an increased speed of rotation was carried out at a speed of (5600 ± 30) min^{-1} for (2 ± 0.1) min.

Measurement of the motor vibration level was carried out in idle mode with a steady speed in the range from (800 ± 30) min^{-1} to (4650 ± 30) min^{-1} on the bearing shield along coordinates X (horizontal axis) and Y (vertical axis) when powered by a traction converter. The root-mean-square value of the vibration velocity in the specified range of rotational speeds should be no more than 2.2 mm/s.

The own level of vibration of the MGU was determined by controlling the rotation by means of an autonomous traction converter with a nominal operating voltage of 3 kV DC and a PWM frequency of 2 kHz.

To determine the level of vibration activity, the ISO 10816 standard allows one of the following values to be used as a measured value [29]:

- vibration displacement, in micrometres (μm);
- vibration velocity, in millimetres per second (mm/s);
- vibration acceleration, in metres per second squared (m/s^2).

According to ISO 10816, the maximum measured vibration level is up to 5 mm/s. in the direction transverse to the output shaft and 2.5 mm/s. in the direction along the output shaft. All components must withstand vibration and shock without damage, according to M27 GOST 30631, sinusoidal vibration with maximum acceleration amplitude of 150 m/s^2 in the frequency range of 0.5–100 Hz. The specified effect is assumed acting from the side of the wheel pair on the wedge plate clutch [30].

Acceptance testing for MGU includes three identical cycles. Parameters such as vibration level, noise, heating temperature of the motor and gearbox bearings in the final – third cycle. At this stage of testing, the main task is to determine the intrinsic vibration activity of MGU and to identify possible resonance through spectral analysis.

The first step is to determine the self-vibration of the first MGU. The scope of dynamic tests consists of three cycles, each of which includes two speed modes – at a continuous speed of 3000 min^{-1} +/– 10 min^{-1} in a clockwise and counterclockwise direction (CW/CCW). Then the rotation speed is increased to the maximal 4653 min^{-1} +/– 10 min^{-1}, and tests are also carried out for two directions of rotation.

The power test bench includes:
- tested MGU (number of gear stages: 2; gear ratio: 5.25; maximum input torque: 3580 Nm; power: 370 kW);
- traction converter, which allows to realize traction drive control modes, the power regulator of which is controlled on the basis of the TMS320F28335 microprocessor;
- autonomous analyser of the level of vibration velocity and vibration acceleration SKF CMXA 80;
- YOKOGAWA WT1800 precision power analyser connected to the output of the traction converter;
- personal computer for the test bench control.

The change in the value of the RMS vibration speed is carried out in the following mode for CW and CCW directions: acceleration – maximal construction speed – maintaining of the maximum speed – braking – coasting – stopping, shown in Fig. 5.3.

The appearance of the maximum value of RMS short-term vibration is acceptable when the design speed is reached and at the initial moment of the motor transition to the braking mode [27].

The test cycle corresponds to the continuous mode S1 with a variable load value. The following example considers the case of deviation from the production technology, identified through the methodology presented in this dissertation. With a decrease in the rotor speed in the coasting mode, vibration cannot depend on the PWM of the traction converter control system and is not associated with the load of the MGU. At the same time, in the coasting mode, the possible presence of resonance can be determined. Figure 5.4 shows a distinct resonance of the traction motor when the rotor speed is within the limited construction speed and at rated speed. The results of the spectral analysis were obtained by means of the fast Fourier transformation. A decomposition of vibration signature leads to speed-dependent motor orders, speed-independent components and speed related off-zero harmonics. The last two components are due to the inverter [32], [33].
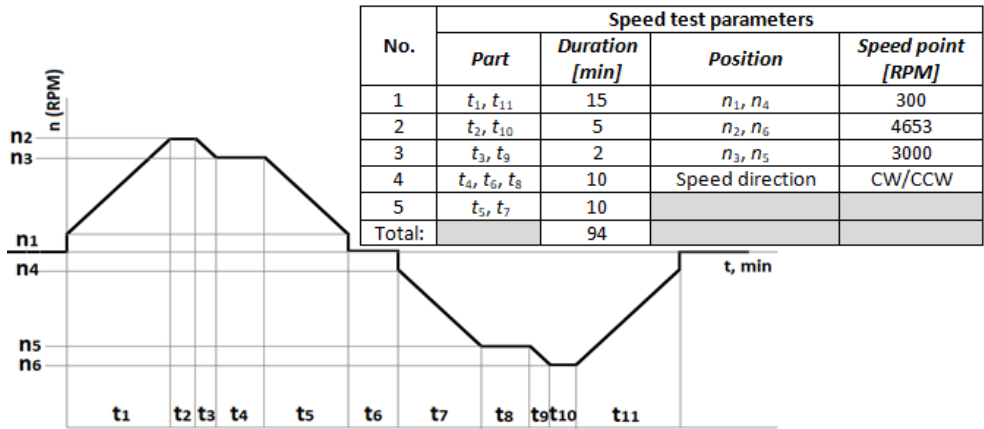
Fig. 5.3. The diagram of the full cycle of MGU dynamic own-vibration test.

No.	Speed test parameters			
	Part	Duration [min]	Position	Speed point [RPM]
1	t_1, t_{11}	15	n_1, n_4	300
2	t_2, t_{10}	5	n_2, n_6	4653
3	t_3, t_9	2	n_3, n_5	3000
4	t_4, t_6, t_8	10	Speed direction	CW/CCW
5	t_5, t_7	10		
Total:		94		
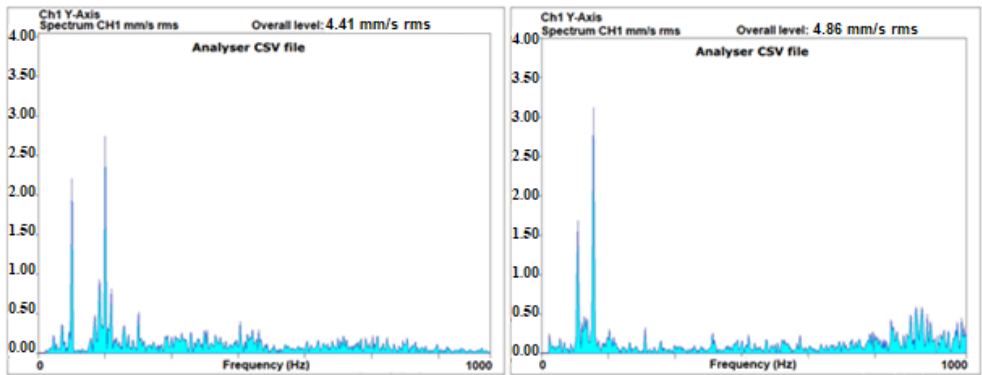
Fig. 5.4. The waveform of the vibration velocity at maximal speed of 4653 min^{-1} and 3000 min^{-1}.

For a rotation speed of 4 653 min^{-1}, in the range of 50.0 – 100.0 Hz (step 1.75 Hz), an increase in the RMS vibration speed up to 4.41 mm/s, in the direction of the Y axis, is fixed. For a rotation speed of 4653 min^{-1}, in the range of 50.0 – 75.0 Hz (step 1.75 Hz), an increase in the RMS vibration speed up to 4.86 mm/s, in the direction of the Y axis, was fixed.

As a result of determining the possible reasons for the appearance of resonance, a violation of the technology of heat treatment of the rotor shaft was revealed, as well as modelling of the shaft stiffness for these conditions was carried out. To ensure the basic hardness of the shaft, the technological process provides for the removal of mechanical stress on the shaft by means of high-temperature tempering at 70 °C for 24 hours. The traction motor shaft has one support and is connected to the gearbox shaft by a flanged diaphragm coupling. The support bearing of the rotor shaft is a single-row ball bearing and does not take axial loads. Shaft deflection in the middle of the rotor is defined as $f = f_g + f_d + f_m$, where f_g is shaft deflection due to gravity, f_d is shaft deflection due to transmission reaction, and f_m is shaft deflection due to magnetic pull [30].

Due to the fact that the profile of the shaft has a stepped configuration, it can be represented by sections and the moment of inertia for each can be determined in accordance with $J_i =$

$\pi d_i^4/64$, where d_i is section diameter. Shaft deflection in the middle of the rotor core due to gravity is $f_g = (G / 3El^2) \cdot (a^2 S_b + b^2 S_a) \cdot 10^6 = 0.0049$ mm, where G is gravity (weight) of the rotor [30]; $E = 2.12 \cdot 10^{11}$ Pa is elastic modulus for 20XH3A steel; and a, b and l are rotor shaft sections, m. The stiffness of the shaft is determined as $k = G / f_g = 0.55 \cdot 10^6$ kgs/cm. The specific magnetic force is $0.0213 \cdot 10^6$ kgs/cm, and the steady-state magnetic attraction force is 3210 N. Further, the fixed value of the vibration acceleration of the MGU corresponding to the test modes will be given with the auto-spectrum of vibration acceleration and vibration velocity with vector control of the PWM. Figure 5.5 shows vibration velocity level at 3 000 min^{-1} on X, Y, Z axes for motor and on Y-axis for gearbox side.
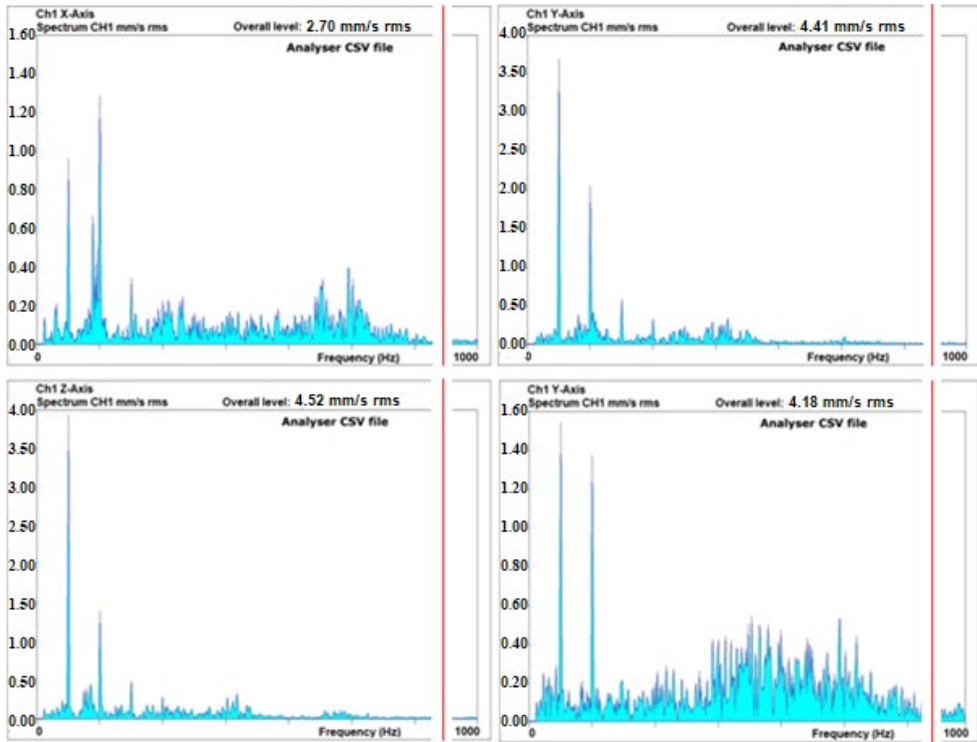
Fig. 5.5. Vibration velocity of MGU fixed at 3 000 min^{-1} on motor bearing shell on X, Y, Z axes and on gearbox shell on the Y-axis.

The fixed values of vibration velocity on Y-axis of 3 000 min^{-1} on motor bearing shell and gearbox side were 4.52 and 4.18 mm/s, which is 1.5 times more than the allowable limit of 2.8 mm/s. Figure 5.6 shows the vibration velocity level at 4653 min^{-1} on X, Y, Z axes for motor and on Y-axis for gearbox side.

The fixed values of vibration velocity on Y axis were 5.84 and 7.92 mm/s, which is more than twice the allowable limit of 2.8 mm/s. Measurements are carried out for 21 control points on the traction motor and gearbox housing along X, Y and Z axes for rotation speeds of 3000 min^{-1} and 4653 min^{-1}.

In an induction motor, the speed is inversely proportional to the load; however, when it is connected to the gearbox, there is certain speed fluctuation. So, it was noticed that with an increase in the rotational speed of the "rotor-shaft MGU" system from 3 000 min^{-1} to

4 653 min^{-1} at the control points, the vibration acceleration average values increase by 1.32 mm/s and 3.74 mm/s, respectively.
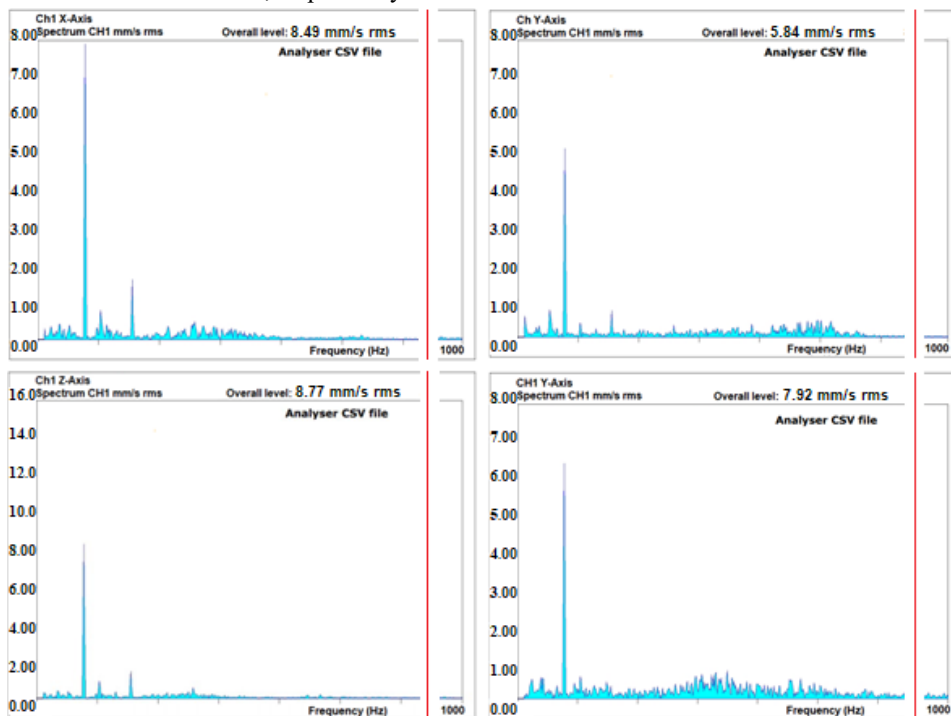
Fig. 5.6. Vibration velocity of MGU fixed at 4 653 min^{-1} on motor bearing shell on X, Y, Z axes and on gearbox shell on Y-axis.

The reason is that the vibration of the gearbox housing, both for the loaded state and in the case of determining its own vibration, is transmitted to the gearbox through a flexible rolling bearing. There is a very strong excitation of the gearbox due to various time-varying parameters such as the gearing stiffness of the tooth, frictional forces and self-torques, as well as the forces of the bearings; thereby causing speed fluctuations [16].

The vibration activity of the intermediate shaft of the gearbox can be most informative when detecting MGU defects at low loads and in case of its absence. All other components change arbitrarily depending on the load.

Figures 5.5 and 5.6 show the spectra of vibration signatures in the range 0–1000 Hz. The frequency range is very important for the study of a transmission gearbox. The level of vibration activity fixed on the Y-axis takes place, and therefore it is reasonable to assume the action of tangential forces arising in magnetic field of the motor (MGU). Excitation of the vibroactivity of the MGU can occur due to the ripple of the torque in closed circuit between the frequency converter and the MGU [28], [30].

Time harmonics are generated by the frequency converter by switching power semiconductors, which in turn can amplify torsional vibrations. Figure 5.7 shows a general view of the location of the MGU on a platform with a spring suspension.

Comparing the results of the spectral analysis of the vibroactivity of the MGU and the control scheme, it can be assumed that the level of the vibrational activity of the MGU decreases when testing under load simultaneously for two MGUs.

Electromagnetic processes in machines are determined by magnetic field in the air gap created by currents flowing along the Y-axis of the machine. The distribution of flux over the air gap of the machine and the change in time ultimately effects the traction and energy characteristics of the traction motor as part of the MGU, as well as its controllability.

In addition, the changing air gap prevents air convection and therefore negatively affects the thermal processes in the winding, increasing the relative temperature difference between the frontal and slot parts of the stator winding.
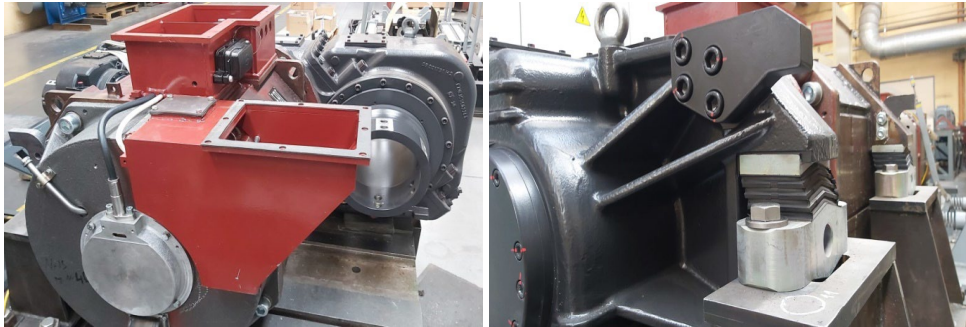
Fig. 5.7. View of MGU from the motor side and from gearbox side.

5.2. Determination of the level of vibration activity of MGU in the mutual load mode

The power converter control controller provides for the implementation of a control system developed within the framework of a model for which a signal form is used and which is recognized by the motor control unit.

In the model, the characteristics of the speed of the electric motor are set, which link the "start-braking" signal with the torque as a function of the angular velocity of the shaft. The velocity ω for the vector control system is used by the feedback signal from the rotor position sensor. The traction and energy characteristics of tested motors are shown in Fig. 3.7. For feedback control, the speed sensor transmits information about the speed of the motor rotor to the speed controller, which is a PI controller with acceleration speed limits, and outputs a reference torque. The torque and magnetic flux are estimated by the observer in accordance with the measured currents and voltages based on equivalent d-q circuits [31]–[34].

The electrical and mechanical systems are connected by the motor rotor. The electrical subsystem generates an electromagnetic moment, which is the input to the mechanical subsystem. The electromagnetic torque at the motor output is one of the inputs for the mechanical state space block (the other input is the torque of the mechanical load). Damping moments and stiffness moments occur along the shaft in couplings, shaft segments and bearings.

To determine the value of the vibration velocity of the MGU under load, two identical MGUs are assembled, the hollow shafts of which are connected by a coupling, and the assembly itself is mounted on a shock-absorbing platform as it is shown in Fig. 5.8. The parameters of the test modes of vibration activity of the MGU under load are the same as given in Fig. 5.8. In the docked state, the middle position of both roller bearings of the traction motors in ensured.

Fig. 5.8. Physical testbench of MGU under the mutual load control.

The characteristics of the change in the auto-spectrum of vibration velocity with vector control of the PWM with constant frequency for rotation speeds of the coupled MGU shafts – 3 000 min^{-1} and 4 653 min^{-1} – are shown in Fig. 5.8. The general level of vibration acceleration in the frequency range 0–1 000 Hz was 0.0990 g at 3 000 min^{-1} and 0.794 g at 4 653 min^{-1}, and the vibration velocity in the frequency range 0–1 000Hz was 1.28 mm/s at 3 000 min^{-1}1 and 1.89 mm/s at 4 653 min^{-1}.

A spectrogram is needed in applications where the vibration frequency changes with time. A spectrogram works by breaking the time domain data into a series of chunks, as it is shown in Fig. 5.9, and taking the FFT of these time periods. These series of FFTs are then overlapped to visualize how both the amplitude and frequency of the vibration signal change with time. Using a spectrogram allows gaining a much deeper understanding of the vibration profile and how it changes with time.
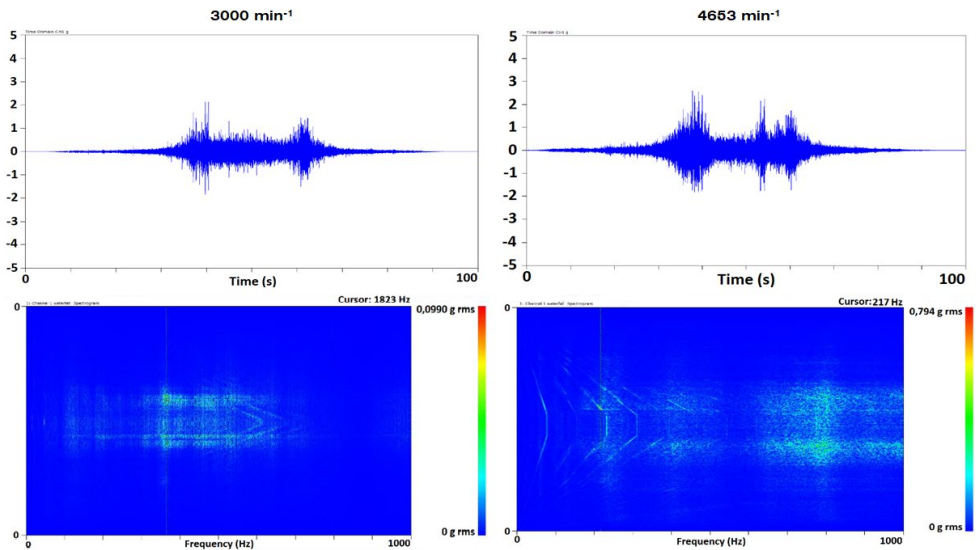
Fig. 5.9. The waveforms and wavefall spectrograms at the rotor speed of 3 000 min^{-1} and 4 653 min^{-1}in Y-axis direction.

RESULTS AND CONCLUSIONS

In the Doctoral Thesis, the dynamics, mechanical strength and technical condition evaluation possibilities of the traction geared motor block were investigated in industrial and continuous production conditions. A methodology was developed that increases the reliability of pre-commissioning tests based on the integrated approach to the control and analysis of mechanical strength and vibration activity of traction equipment.

The developed methodology is based on real peculiarities of the technological process of production, as well as on real working conditions of the equipment, taking into account the mechanical loads of the traction drive.

In the course of the Thesis research, a strength calculation of the zones of maximal stress of the gearbox was performed under various loads, including shock loads. The analysis of the safety margin of the bearing structure of the traction gear was carried out. According to the results of the calculation, by means of a physical experiment, the level of vibration activity of the structure of the gearbox as part of the MGU and controlled by the original voltage and frequency converter was established. The experimentally determined indicators of the vibration activity of the gearbox in the loaded state make it possible to confirm the simulated strength and stability of the structure to the effects of external purely mechanical disturbances and mechanical disturbances caused by electromagnetic phenomena of the traction drive.

It is recommended to carry out an autonomous check of traction single-support motors for mechanical strength before their docking with the gearbox. The tests carried out relate to the MGU in which the geometry of the flange and the gearbox housing ensure the middle position of the roller bearing of the motor, which is the most favourable from the point of view of reducing vibration activity. When the rollers are displaced relative to the middle position, the vibration activity indicators will deteriorate, while the bearing heating temperature will increase.

The presence of resonance of the rotating system "motor rotor – gearbox input shaft" in the range of rotation speeds close to the nominal leads to long-term sustained oscillating processes at the output shaft of the MGU and increased vibration. The main task in the design and manufacture of MGU is to exclude resonant frequencies from the range of nominal operating speeds.

The changing level of vibration velocity in the direction of the Y-axis is the determining value when controlling the strength-vibration, noise and thermal parameters of MGU. The data obtained make it possible to identify the zone of dangerous resonance of the MGU design from the point of view of electromechanical resonances and suggest ways to control the state of the MGU nodes.

To calculate the strength data of MGU nodes, an experimental evaluation of the amplitude-frequency characteristics obtained on the MGU body was carried out. The limit values of the vibration frequency for MGU are 26–33 % of the maximum allowable value.

It is revealed that the vibration is continuous in time and corresponds to spectrum of the broadband region. In addition to vibration caused by external causes (from the upper structure of the track), vibrations that occur during the operation of the drive act on the wheel-motor unit of the electric train, which under certain conditions causes shock vibrations, and this significantly increases the amplitude of vibrations of its local parts.

The results of vibration research during testing of the MGU of a suburban electric train in traction mode and with shock load removal are obtained and presented.

The experimental measurements carried out confirm the calculated strength of MGU and determine the frequency spectrum under shock loads.

The vibration of the gearbox housing, both for the loaded state and in the case of determining its own vibration, is transmitted to the gearbox through a flexible rolling bearing. There is a more powerful excitation of the gearbox due to time-varying parameters such as the gearing stiffness of the tooth, frictional forces and self-torques, as well as the forces of the bearings; thereby causing speed fluctuations. For example, a vibration level fixed on the Y-axis may be due to shear forces generated in the motor magnetic field. Also, the existing vibration excitation of the MGU can occur due to the torque pulsation in a closed circuit between the frequency converter and the MGU twin. Temporal harmonics are generated by the frequency converter by switching power semiconductors, which in turn can amplify torsional vibrations.

Considered as an example, the design of MGU meets the requirements of design reliability in terms of critical parameters of mechanical rigidity and short-term shock loads. However, due to the presence of a large number of bolted connections in the design, each manufactured unit of the MGU must undergo acceptance tests to check the level of vibration activity and also be subjected to careful control during operation.

The cast-iron casing of the MGU with axial-support suspension and the fastening of the traction motor flange to the gearbox casing flange ensure the rigidity of the structure and meet the requirements of extremely high external mechanical influences. With a high level of vibration and single shocks, the operation of the MGU will be characterized by increased wear of the gears of the reducer and the thrust bearing of the traction motor.

LIST OF REFERENCES

1. Горелик, А. Л. Методы распознавания / А. Л. Горелик, В. А. Скрипкин. – М.: Высшая школа, 1977. – 22 с.

2. Sendhil Kumar, S.; Senthil Kumar, M. Condition monitoring of rotating machinery through vibration analysis. J. Sci. Ind. Res. 2014, 73, 258–261.

3. Русов, В. А. Диагностика дефектов вращающегося оборудования по вибрационным сигналам / В. А. Русов. – Пермь: Изд-во "Вибро-Центр", 2012. – 244 с.

4. Hou, D.; Qi, H.; Luo, H.; Wang, C.; Yang, J. Comparative study on the use of acoustic emission and vibration analyses for the bearing fault diagnosis of high-speed trains. Struct. Health Monit. 2021, 14759217211036025. https://doi.org/10.1177/14759217211036025

5. ISO 17359:2018 Condition monitoring and diagnostics of machines – General guidelines, p. 29.

6. ISO 13380:2002 Condition monitoring and diagnostics of machines – General guidelines on using performance parameters, p. 19.

7. ISO 13379-1:2012 Condition monitoring and diagnostics of machines – Data interpretation and diagnostics techniques – Part 1: General guidelines, p. 33.

8. ISO 10816-8:2014 Mechanical vibration – Evaluation of machine vibration by measurements on non-rotating parts, p. 27.

9. ISO 13373-1:2002 Condition monitoring and diagnostics of machines – Vibration condition monitoring – Part 1: General procedures, rev. 2018, p. 51.

10. ISO 15242-1:2015 Rolling bearings – Measuring methods for vibration – Part 1: Fundamentals, rev. 2021, p. 16.

11. ISO 13374-3:2012 Condition monitoring and diagnostics of machines – Data processing, communication and presentation – Part 3: Communication, rev. 2017, p. 21.

12. Сиротин, Д. В. Использование параметров токового сигнала электродвигателя для оценки технического состояния электромеханического оборудования / Д. В. Сиротин // Известия высших учебных заведений. Северо-Кавказский регион. Технические науки, 2006. – С. 57–62.

13. Чернов, А. В. Обработка диагностической информации при оценке технического состояния электроприводной арматуры АЭС / А. В. Чернов, О. Ю. Пугачёва, Е. А. Абидова // ИВД, 2011. – №3. – С. 337–342.

14. Gelman, L.; Kolbe, S.; Shaw, B.; Vaidhianathasamy, M. Novel adaptation of the spectral kurtosis for vibration diagnosis of gearboxes in non-stationary conditions. Insight Non-Destr. Test. Cond. Monit. 2017, 59, 434–439. https://doi.org/10.1784/insi.2017.59.8.434

15. Isham, M. F.; Leong, M. S.; Hee, L. M.; Ahmad, Z. A. B. Iterative variational mode decomposition and extreme learning machine for gearbox diagnosis based on vibration signals. J. Mech. Eng. Sci. 2019, 13, 4477–4492. https://doi.org/10.15282/jmes.13.1.2019.10.0380

16. Mauricio, A.; Zhou, L.; Mba, D.; Gryllias, K. Vibration-Based Condition Monitoring of Helicopter Gearboxes Based on Cyclostationary Analysis. J. Eng. Gas Turbines Power 2020, 142, 031010. https://doi.org/10.1115/1.4044453

17. Барков, А. В. Идентификация состояния механизмов с узлами вращения по результатам вибрационного мониторинга и контроля температуры. Методика

МВ.03.7826741252./23.12.2011 / А. В. Барков, Н. А. Баркова, Д. В. Грищенко. – Санкт-Петербург, 2011. – 80 с.

18. All about Vibration Measuring Systems. Vibration Technical guide // el. resource: https://www.imv.co.jp/e/pr/vibration_measuring/chapter03/ (last visit: 12.08.2022)

19. Huang, S.; Zheng, J.; Pan, H.; Tong, J. Order-statistic filtering Fourier decomposition and its application to rolling bearing fault diagnosis. JVC J. Vib. Control 2021, 1–16. https://doi.org/10.1177/1077546321997598

20. Hartono, D.; Halim, D.; Roberts, G. W. Gear fault diagnosis using the general linear chirplet transform with vibration and acoustic measurements. J. Low Freq. Noise Vib. Act. Control 2019, 38, 36–52. https://doi.org/10.1177/1461348418811717

21. Guoji, S.; McLaughlin, S.; Yongcheng, X.; White, P. Theoretical and experimental analysis of bispectrum of vibration signals for fault diagnosis of gears. Mech. Syst. Signal Process. 2014, 43, 76–89. https://doi.org/10.1016/j.ymssp.2013.08.023

22. Kawada, M.; Yamada, K.; Yamashita, K. Fundamental Study on Vibration Diagnosis for High-Speed Rotational Machine using Wavelet Transform. IEEJ Trans. Power Energy 2003, 123, 1229–1241. https://doi.org/10.1541/ieejpes.123.1229

23. Stander, C. J.; Heyns, P. S.; Schoombie, W. Using vibration monitoring for local fault detection on gears operating under fluctuating load conditions. Mech. Syst. Signal Process. 2002, 16, 1005–1024. https://doi.org/10.1006/mssp.2002.1479

24. Ocak, H.; Loparo, K. A. A new bearing fault detection and diagnosis scheme based on hidden Markov modeling of vibration signals. In: Proceedings of the ICASSP, IEEE International Conference on Acoustics, Speech and Signal Processing-Proceedings, Salt Lake City, UT, USA, 7–11 May 2001; Volume 5, pp. 3141–3144. https://doi.org/10.1109/ICASSP.2001.940324

25. Betta, G.; Liguori, C.; Paolillo, A.; Pietrosanto, A. A DSP-based FFT-analyzer for the fault diagnosis of rotating machine based on vibration analysis. IEEE Trans. Instrum. Meas. 2002, 51, 1316–1321. https://doi.org/10.1109/TIM.2002.807987

26. Русов, В. А. Спектральная вибродиагностика / В. А. Русов. – Пермь: Изд-во "Вибро-Центр", 1996. – 176 с.

27. Зайцев, А. В. Определение возможности уменьшения числа датчиков вибрации при диагностировании колесно-моторных блоков электропоезда / А. В. Зайцев, А. А. Лагаев, В. Н. Костюков //Наука, образование, бизнес: регион. науч. – практ. конф. – Омск, 2009. – С.154 – 157.

28. Dvornikov, I., Marinbahs, M., Sliskis, O., Ketners, K. "Investigation of autonomous traction motor dynamic using method of mutual loading and computer simulation" in *2018 IEEE 59th International Scientific Conference on Power and Electrical Engineering of Riga Technical University (RTUCON)*, Riga, Latvia, 2018.

29. Kobenkins, G., Marinbahs, M., Burenin, V., Zarembo, J., Sliskis, O. "Carrying Out of Strenght Tests of Geared Motor Box as Part of a Frequency-Controlled Traction Electric Drive" in *2021 17th Conference on Electrical Machines, Drives and Power Systems (ELMA)*, Sofia, Bulgaria, 2021.

30. Dvornikov, I., Marinbahs, M., Kobenkins, G., Sliskis, O., Ketners, K. "Carrying out Tests for the Functionality of the Traction Autonomous Drives in the Conditions of Industry and Serial Production" in *2021 17th Conference on Electrical Machines, Drives and Power Systems (ELMA)*, Sofia, Bulgaria, 2021.

31. Kobenkins, G., Marinbahs, M., Burenin, V., Zarembo J., Bizans, A., Sliskis, O. "Determination of the Level of Own Vibration of Geared Motor Boxes in Industrial Conditions" in *2021 IEEE 62nd International Scientific Conference on Power and Electrical Engineering of Riga Technical University (RTUCON)*, Riga, Latvia, 2021.

32. Kobenkins, G., Marinbahs, M., Bizans, A., Rilevs, N., Burenin, V., Sliskis, O. "Carrying Out of Strength Control of Mutual Loaded Traction Geared Motor Boxes as a Part of Industrial Tests" in *2022 9th International Conference on Electrical and Electronics Engineering (ICEEE)*, Alanya, Turkey, 2022.

33. WIKOV MGI // Technical report, Hronov 2020, p. 57.

33. Marinbahs, M., Kobenkins, G., Pavelko, V. Bizans, A., Rilevs, N., Sliskis, O. "Determination of the Strength Characteristics of Traction Gears Under Shock Loads" in the 8th International Youth Conference on Energy (IYCE-2022) 6–9 July 2022, Eger, Hungary.

34. Kobenkins, G., Marinbahs, M., Bizans, A., Rilevs, N., Burenin, V., Sliskis, O. "Evaluation of the Strength of Traction Geared Motor Units by Permissible Stresses and the Level of Vibration Activity" in Proc. of the International Conference on Electrical, Computer and Energy Technologies (ICECET 2022) 20–22 July 2022, Prague, Czech Republic.
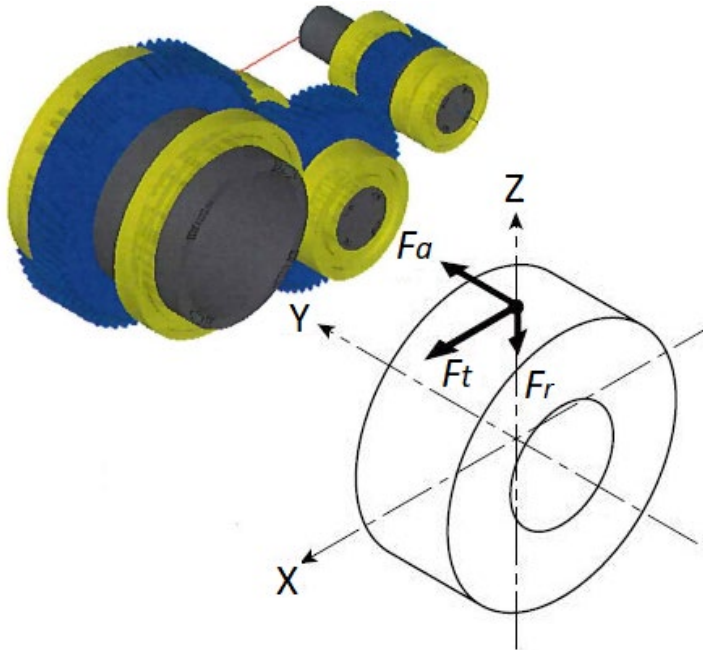
Direction of Forces Acting on a Gear.

The force that acts in the *X*-axis direction is defined as tangential force F_t (N).

The force that acts in the *Y*-axis direction is defined as axial force F_r (N).

The force that acts in the *Z*-axis direction is defined as radial force F_x (N).
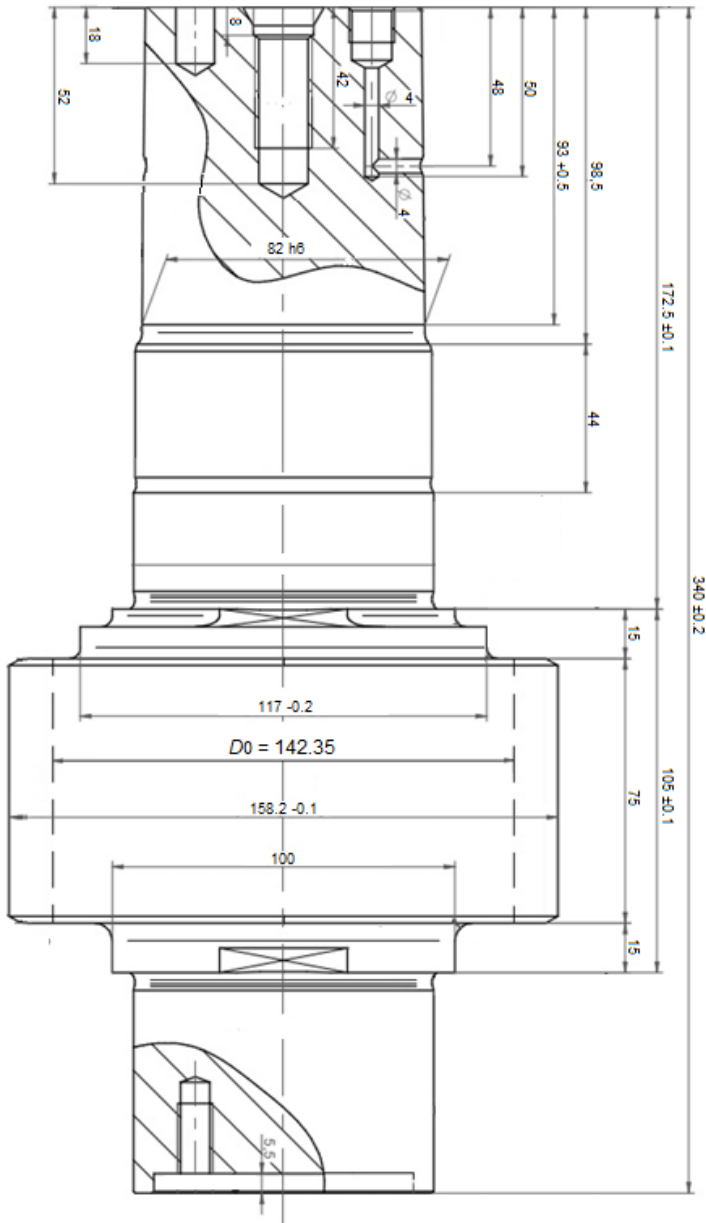
Pitch circle diameter D_0